

國立交通大學

電機與控制工程學系

碩士論文

具有偵測內部電阻補償電路及平穩控制技術的
鋰離子電池快速充電器之研究設計

Li-Ion Battery Charger with Smooth Control Circuit
(SCC) and Built-in Resistance Compensator (BRC) for
Achieving Stable and Fast Charging

研究生：林家祥

指導教授：陳科宏 博士

中華民國九十七年九月

具有偵測內部電阻補償電路及平穩控制技術的

鋰離子電池快速充電器之研究設計

Li-Ion Battery Charger with Smooth Control Circuit (SCC) and
Built-in Resistance Compensator (BRC) for Achieving Stable and Fast
Charging

研究生：林家祥

Student：Chia-Hsiang Lin

指導教授：陳科宏

Advisor：Ke-Horng Chen

國立交通大學
電機與控制工程學系

碩士論文

A Thesis

Submitted to Department of Electrical and Control Engineering
College of Electrical Engineering
National Chiao Tung University
in partial Fulfillment of the Requirements
for the Degree of
Master
in

Electrical and Control Engineering

September 2008

Hsinchu, Taiwan, Republic of China

中華民國九十七年九月

具有偵測內部電阻補償電路及平穩控制技術的

鋰離子電池快速充電器之研究設計

研究生：林家祥 指導教授：陳科宏博士

國立交通大學電機與控制工程研究所碩士班

摘要

在科技日益進步的這幾年之間，可攜式產品已經成為了人人不可或缺的必備工具，諸如手機、PDA 或是數位相機等，都成為了市場上主要的消費產品。而在這許多的應用之中，限制其使用的最主要原因就是電池的效能。

配合可攜式產品的發展，可充電電池的重要性亦大幅增加。如何安全並且快速的充電，就成為了一項很重要的議題。近幾年間，充電電池都採用了定電流-定電壓(CC-CV)充電法。當充電器對一顆放電完畢的電池充電時，會先以小電流對電池進行儲能的動作。當電池電壓上升至一個較高的位準時，充電器便以大電流進行快速的充電。當電池充至一個預先的額定電壓位準(ex: 4.2V)時，便進入了定電壓模式。然而因為電池本身以及充電器上的寄生電阻，會讓電池的能量並未完全儲滿。為了令電池達到最大的儲能量，在定電壓模式中充電器提供了一個漸漸下降的電流來補足能量。當電流下降至足夠微小時，便停止充電，此時就完成了一個完整的充電週期。

在充電過程中，定電流模式跟定電壓模式的轉態點以及定電壓模式的時間決定了充電的週期長短。在定電流以及定電壓的轉態過程中，若是採用數位控制便容易產生電池電壓震盪而處於不穩定的狀態。同時在定電壓的衰減電流充電過程中，亦會相對延長充電時間。為了改善此兩項缺點，本篇論文提出一個包含了 SCC 以及 BRC 的充電器架構。不僅令充電器能平順的切換工作模式，同時加速了充電週期。本論文使用了 TSMC 0.35 μ m2P4M 製程，而實驗結果亦顯示了出明顯的改善。

Li-Ion Battery Charger with Smooth Control Circuit (SCC) and Built-in Resistance Compensator (BRC) for Achieving Stable and Fast Charging

Student: Chia-Hsiang Lin Advisor: Dr. Ke-Horng Chen

Department of Electrical and Control Engineering
National Chiao-Tung University

Abstract

A built-in resistance compensator (BRC) to speed up the charging time of the lithium-ion (Li-Ion) battery is presented and experimentally verified in this paper. Based on the physical properties of the battery cell, the charger charges the cell with three stages, which are trickle current (TC), constant current (CC), and constant voltage (CV) stages [1], [2].

When the battery is under the low voltage, ex: 2.5V, the structure of the battery system pack is easy to be damaged from the large charging current. That is the reason the charger charges the Li-Ion cell by trickle current but prolongs the whole charging process. Once the voltage of battery reaches the specified value, 2.5V, the charger then switches to the constant current stage and charges the battery in larger current to fasten the charging speed. At the end of the constant current stage, the battery reaches the rated voltage (ex: 4.2V) and the charger enters the constant voltage stage.

A smooth control circuit (SCC) is proposed to ensure the stable transition from the CC stage to the CV stage. The charger keeps the voltage of the battery in stable level until the charger stops the whole charging process. However, due to the external parasitic resistance of the Li-Ion battery pack system, the charger circuit switches from the CC stage to the CV stage without fully charging the cell to the rated voltage value. The Li-Ion cell is needed to be charged by a degrading current at the CV stage to avoid overcharging. The longer the cell stays at the CV stage, the longer the charging time is owing to the degrading current. The BRC technique can dynamically estimate the external resistance of the battery pack system to extend the period of the CC stage. The test chip was fabricated in TSMC 0.35- μm technology. Experimental results show that the period of the CC stage can be extended to about 40% that of the original design. The charging time can be effectively reduced.

誌 謝

論文終於完成了，在這完筆的時刻，心中有特別多的感謝。首先最要感謝的，就是我的指導老師陳科宏博士。從我踏入大學之際，就受到了老師對我的關切指導，在進入了研究所之後，老師更是帶領了我進入類比 IC 設計更為深入的領域，在學業研究的同時，也教會了我許多做人處事的道理。能夠在這六年期間遇到陳科宏老師，我心裡充滿了感激。另外我也要感謝論文口試的評審委員，王清松教授和黃立仁博士的寶貴意見，使本論文內容能夠的更加完整。

同時，我要感謝博士班的宏瑋學長，在電路設計上對我的指導以及相關領域的指點，從學長的身上我學到了許多類比 IC 設計上的重要觀念。另外還要感謝我六年來的好同學—謝俊禹，從大學時就給予了我許多的幫助，進入了研究所之後，更是不吝惜的將相關經驗與我分享，使我能夠在課業上有好的表現。再來，我要感謝研究所的好伙伴—Aga、韋任、VaLuE、歪歪，與你們一起奮鬥的日子，是我研究所最珍貴的回憶。還要感謝小柯、國林、逢哥，因為有你們的指導，才能讓我在Layout的領域有所進步，非常的謝謝你們。再來要謝謝802、701、703實驗室的老同學在我這段時間的協助，有你們的幫忙才能使論文順利的完成。還有要感謝我大學時期的好朋友—李泰、哲嘉、馬橋、江爺、小豪、百毅、楨哥哥、Hank，因為有你們陪我一起玩樂、一起聊天、讓我在研究的過程中減輕了許多壓力。

感謝我的女友小P，在這段時間對我的包容與陪伴，讓我能專心的朝著目標邁進。最後我要謝謝我的父母以及家人，因為有你們的支持，我才能無後顧之憂的研讀學業，攻讀碩士學位，我會帶著你們的關懷，在未來的路上繼續努力。

謹以此篇論文獻給我身邊的每位好朋友

Contents

CHAPTER 1	1
INTRODUCTION	1
1.1 INTRODUCTION TO RECHARGEABLE BATTERY	2
1.2 THE BASIC CONCEPT OF THE LI-ION BATTERY	5
1.3 THE PACKAGE OF THE CHARGER	7
1.4 MOTIVATION	9
CHAPTER 2	11
THE BASIC CONCEPT OF THE CONVENTIONAL CHARGER AND THE PRIOR CC-CV CHARGER	11
2.1 THE CONCEPT OF THE CHARGING METHOD FOR NI-BASED BATTERY AND LI-BASED BATTERY	12
2.1.1 <i>The Voltage-Controlled Charging Method for Ni-MH, Ni-Cd battery</i>	12
2.1.2 <i>The Constant Current to Constant Voltage Charging Method for Li-Ion Battery</i>	14
2.2 THE PROPERTIES OF THE CONVENTIONAL CHARGER	17
2.2.1 <i>The Unstable Transition of CC to CV Stage</i>	17
2.2.2 <i>The Short Duration of the CC Stage</i>	19
2.3 THE PRIOR ART AND THE PROPOSED METHOD	21
2.3.1 <i>The Analogy Transition Method to CC Stage and CV Stage</i>	21
2.3.2 <i>The Solution to the Early Entrance of the CV Stage</i>	23
CHAPTER 3	24
THE CIRCUIT IMPLEMENTATION OF BRC AND SCC TECHNIQUE AND SIMULATION RESULT	24
3.1 THE IMPLEMENTATION AND SIMULATION OF SCC (SMOOTH CONTROL CIRCUIT) TECHNIQUE	25
3.2 THE CIRCUIT CONCEPT, IMPLEMENTATION, AND SIMULATION OF BRC TECHNIQUE	27
3.2.1 <i>The Concept of BRC Technique</i>	27
3.2.2 <i>The Estimation of the External Resistance at the CC Stage</i>	29
3.2.3 <i>The Proposed Architecture of the Charger with the BRC Technique</i>	30
3.2.4 <i>The Proposed External Resistance Detector and the Reference Voltage Switch Circuit</i>	35
3.2.5 <i>The Proposed Reference Shift Circuit</i>	40
3.3 THE WHOLE CIRCUIT SIMULATION OF THE CHARGER WITH BRC TECHNIQUE	44
CHAPTER 4	45
THE ENVIRONMENTAL SET-UP AND THE MEASUREMENT RESULTS OF THE CHARGER WITH BRC	45
4.1 THE ENVIRONMENTAL SET-UP AND CHIP MICROGRAPH OF THE BRC CHARGER	45

4.2 THE MEASUREMENT RESULTS OF THE CHARGER	48
CHAPTER 5	51
CONCLUSIONS AND FUTURE WORKS.....	51
5.1 CONCLUSIONS	51
5.2 FUTURE WORKS	52
REFERENCES	53
ISSUED PAPER LIST	56



FIGURE CAPTIONS

Fig. 1 A statistics of sales in the market of several kinds of batteries	3
Fig. 2 The real structure of the Li-Ion battery	5
Fig. 3 The equivalent circuit of battery	6
Fig. 4. The whole package of the charger IC and battery	7
Fig. 5. The simplified circuits of the charger IC and battery.....	8
Fig. 6. The charging waveform of the Ni-MH and Ni-Cd battery.....	13
Fig. 7. The conceptual structure of the basic charger circuit.....	15
Fig. 8. The waveform of the unstable transition between the CC and CV stages due to the IR-drop voltage of the battery pack.....	18
Fig. 9. The IR-drop voltage under the different charging current and R_{pack} . (a) The IR-drop voltage is affected by the product of the charging current and the external resistance. (b) The charging timing diagrams of points A and B in (a).	20
Fig. 10. The simplified diagram of the charger based on the analogy method.....	22
Fig. 11. The improved waveform of the charger with SCC technique.....	25
Fig. 12. The drain current of the transistors M_{VA} and M_2	26
Fig. 13. The improved waveform at the end of charging process after using the BRC technique.....	28
Fig. 14. The proposed fast-charging charger with the external resistance estimation.....	30
Fig. 15. The waveform of battery voltage during detecting period.....	32
Fig. 16. The waveform of V_{BAT} , V_{BATO} , V_{SET}' , and I_{CHRG} during the detection period, $R_{pack}=150m\Omega$	33
Fig. 17. The waveform of V_{BAT} , V_{BATO} , V_{SET}' , and I_{CHRG} during the detection period, $R_{pack}=300m\Omega$	34
Fig. 18. (a) The schematic of the circuit of external resistance detector with an on-chip sample-and-hold circuit. (b) The schematic of the delay line circuit.	36
Fig. 19. The waveform of V_{BAT}' and V_1' during the detection period.....	37
Fig. 20. The waveform of V_{BAT}' and V_2' during the detection period, (a) $R_{pack}=150m\Omega$, (b) $R_{pack}=300m\Omega$	38
Fig. 21. The 9-bit digital code of the delay line circuit, (a) $R_{pack}=150m\Omega$, (b) $R_{pack}=300m\Omega$..	39
Fig. 22. The reference shift circuit generates the BRC reference voltage V_{REF}' by adding the increment voltage V_{INC} to the original reference voltage V_{REF}	40
Fig. 23. The waveform of the digital bits, 0000000001 and compensated V_{REF}' for IR-drop..	42
Fig. 24. The waveform of the digital bits, 1111111111 and compensated V_{REF}' for IR-drop...	43
Fig. 25. The whole circuit simulation of the charger with BRC technique.....	44

Fig. 26. The estimation set-up of the proposed charger.....46

Fig. 27. Chip micrograph.....47

Fig. 28. The smooth charging waveform from the CC to CV stage achieved by the analogy method.48

Fig. 29. The waveforms of the voltage V_{BATO} w/i and w/o the BRC technique. The CC stage of the original design is extended to the CC' stage of the BRC design.49

Fig. 30. The waveforms of the voltages V_{BAT} and V_{BATO} w/i and w/o the BRC technique. The voltages of the compensated V_{BAT} and V_{BATO} are got from the BRC technique..... 50

Fig. 31. The waveform of the voltage V_{SET} during the detection period. 50



Table Captions

TABLE I DIFFERENT TYPES OF RECHARGEABLE BATTERY	2
TABLE II THE ADVANTAGES AND DISADVANTAGES OF EACH TYPE OF RECHARGEABLE BATTERY	3
TABLE III THE THREE OPERATING MODE OF THE CONVENTIONAL CHARGER	15
TABLE IV THE CORRESPONDING VALUES TO THE VOLTAGE, V_{INC} OF DISTINCT EXTERNAL RESISTANCE, R_{PACK}	41
TABLE V: SPECIFICATIONS OF THE PROPOSED CHARGER WITH THE BRC TECHNIQUE	46



Chapter 1

Introduction

The portable devices, such as PDAs, cell-phones, digital cameras etc., have become the most popular applications in recent years [3]. Among these electrical manufactures, the battery-operated device is the main issue to the power management area. The main characteristic of the portable devices is the utilization of rechargeable battery. Due to the features of light weight, small size, and high energy density, the rechargeable batteries are widely used in the portable applications.

However, the energy stored in the battery is corresponding to the diverse materials. Besides, the other properties such as life cycles, self-discharge rate etc., could affect the performance of the rechargeable battery. In summation, the rechargeable battery plays an important role in the portable products. Furthermore, because of the limitation of the energy capacity of the battery, the using time of the electrical product is limited. In order to reach the longer using time, employing the energy of the battery economically is stringent to power-saving issue.

Chapter 1 is divided into four sections. Section 1.1 introduces the fundamental concepts of the rechargeable battery and lists the comparison of different types of battery. Section 1.2 introduces the basic concept of the Li-Ion battery. Section 1.3 introduces the package of the charger and section 1.4 illustrates the motivation of the proposed circuit in this paper.

1.1 Introduction to Rechargeable Battery

Nowadays, the portable devices have become the main applications of advanced technical products. Owing to the many advantages of the rechargeable battery, there are many types of that developed to meet the requirement of the expanding market. The characteristics of some most popular rechargeable battery, ex: Ni-MH, Ni-Cd, Li-Ion batteries are listed in TABLE I. The performance of the rechargeable battery is judged by many aspects inclusive of operating voltage, specific energy, energy density, cycle life, self-discharge rate, etc. The specific energy represents the stored energy of the different types of charger under the same weight. The energy density implies that the energy stored in the battery under the same volume. The cycle life means the number of times of discharging of the rechargeable battery [4]. Among these factors, the most important feature of the rechargeable battery is the self-discharge rate. The self-discharge rate stands for the leakage energy per month of the battery under the non-using condition. TABLE I shows the comparison of the often seen batteries [5]. TABLE II lists the advantages and disadvantages of each type of rechargeable battery.

TABLE I

DIFFERENT TYPES OF RECHARGEABLE BATTERY

<i>Battery Type</i>	<i>Operating Voltage (V)</i>	<i>Specific Energy (Wh.kg⁻¹)</i>	<i>Energy Density (Wh.L⁻¹)</i>	<i>Cycle Life (times)</i>	<i>Self-discharge Rate (%.per month)</i>
<i>Li-Ion Polymer</i>	<i>3.7</i>	<i>120-170</i>	<i>300-460</i>	<i>≥1000</i>	<i>≤3</i>
<i>Li-Ion</i>	<i>3.6</i>	<i>100-160</i>	<i>270-360</i>	<i>1000</i>	<i>6-9</i>
<i>Ni-Zn</i>	<i>1.65</i>	<i>60-75</i>	<i>240</i>	<i>500</i>	<i>-</i>
<i>Ni-MH</i>	<i>1.2</i>	<i>65</i>	<i>200</i>	<i>500</i>	<i>30-35</i>
<i>Lead-acid</i>	<i>2</i>	<i>25-45</i>	<i>80-100</i>	<i>250-450</i>	<i>-</i>
<i>Ni-Cd</i>	<i>1.2</i>	<i>30-50</i>	<i>150</i>	<i>500</i>	<i>25-30</i>

TABLE II
THE ADVANTAGES AND DISADVANTAGES OF EACH TYPE OF RECHARGEABLE BATTERY

<i>Battery Type</i>	<i>Advantages</i>	<i>Disadvantages</i>
<i>Li-Ion Polymer</i>	<i>High specific energy and energy density, long life</i>	<i>High cost, limited capacity and discharging rate</i>
<i>Li-Ion</i>	<i>High specific energy and energy density, long life</i>	<i>High cost, complexity of operation circuit, heating at high discharging rate</i>
<i>Ni-Zn</i>	<i>New technology, high specific energy and energy density</i>	<i>Few commercial products</i>
<i>Ni-MH</i>	<i>High specific energy and energy density, acceptable cost</i>	<i>Limited charging rate</i>
<i>Lead-acid</i>	<i>Widely used and low cost</i>	<i>Low specific energy and energy density, environmental concerns</i>
<i>Ni-Cd</i>	<i>Stable discharging voltage, high discharging rate</i>	<i>Serious environmental concerns</i>

The Ni-MH and Ni-Cd batteries were the chief batteries in the handheld device before. However, it is obvious that the Li-Ion battery is superior to other type referred to TABLE II. As Fig. 1 shown, the use of Li-Ion battery takes the replace of mentioned battery in recent years. The sales of Li-Ion batteries have increased sharply since 1992 [6].

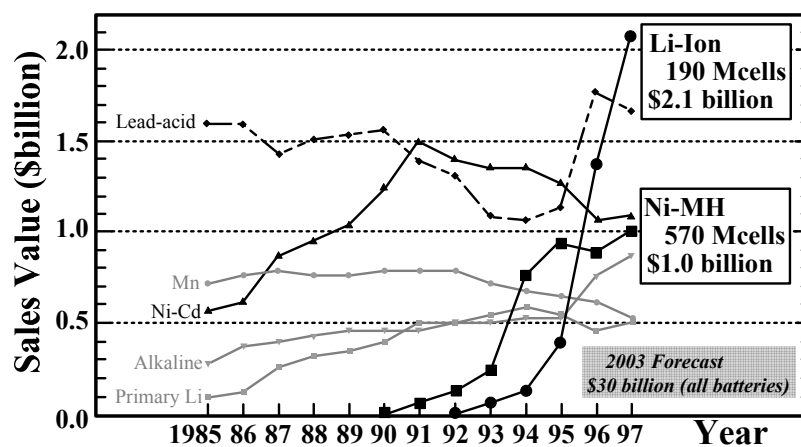


Fig. 1 A statistics of sales in the market of several kinds of batteries

The specific energy and the energy density of Li-Ion battery are double than that of Ni-Zn and Ni-Cd batteries. The more important is that the long cycle life characteristic of the Li-Ion battery. Another major quality about the Li-based battery is the memory effect. The more accurate term of the memory effect is the voltage depression. For the Ni-Cd battery, the energy capacity of the cell is affected by the depth of discharge. When the battery is not fully discharged, the battery remember the shorten cycle and reduce the capacity. However, according to the relative research of the Li-Ion battery, the deep discharge of the Li-Ion battery shortens the life cycles contrarily.

Based on the fact, the Li-Ion battery is chose to be the main subject in this paper. Nevertheless, the limit of the life cycles is the critical problem to the Li-Ion battery. The life cycles are easily affected by undercharging or overcharging issues [7], [8]. The reason is that the overcharging issue may damage the physical component of the battery. On the other hand, the undercharging issue may reduce the energy capacity of the battery. Therefore, this paper proposed the new circuit to enhance the performance of Li-Ion battery charger in many aspects, whether the life cycles or the charging speed.

1.2 The Basic Concept of the Li-Ion Battery

The advantages of the Li-Ion battery include high energy density, long cycle life, low self-discharge rate, and no memory effect referring to the TABLE I. It has become the major battery for the portable and wireless products. In order to improve the performance of the Li-Ion battery, the basic knowledge of the battery is needed. The Li-Ion battery is comprised of the carbon anode and a Lithia-cobalt dioxide or manganese dioxide cathode with a liquid or solid electrolyte separator as Fig. 2 shows. The equation (1) \ (2) are the reaction equations of the Li-Ion battery.

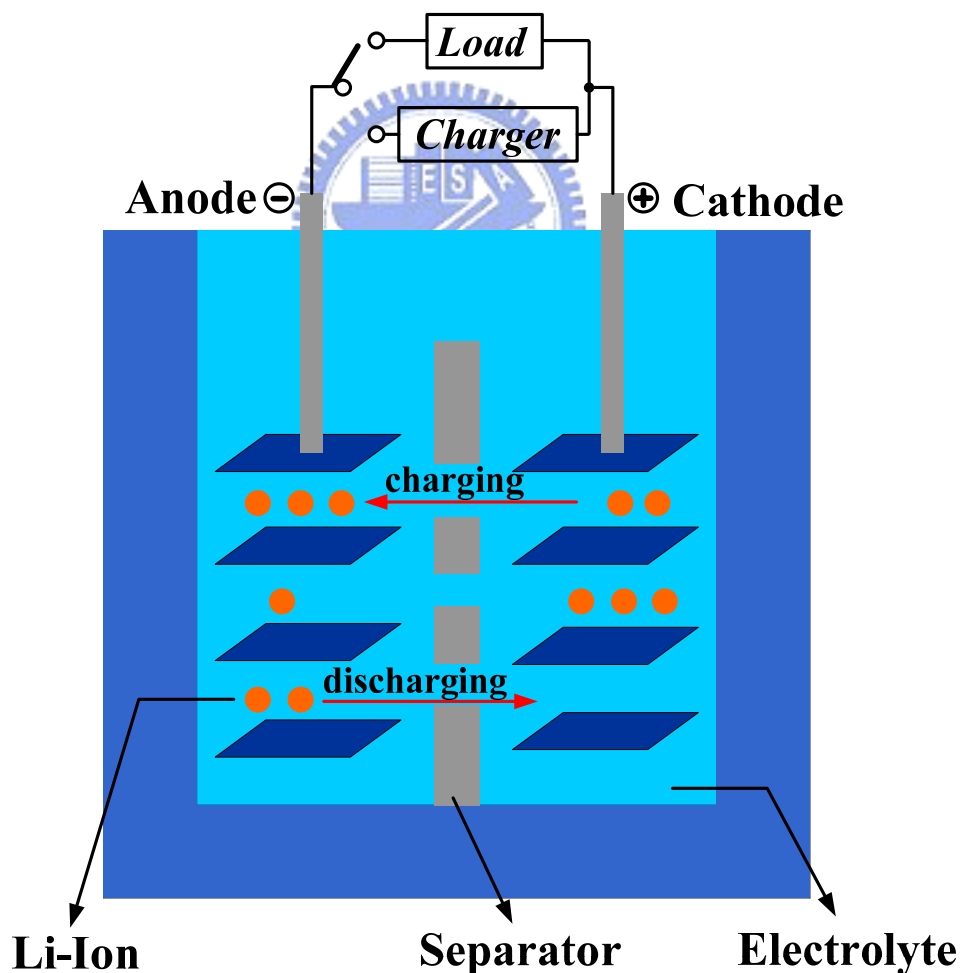
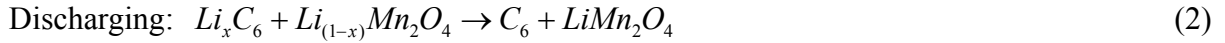
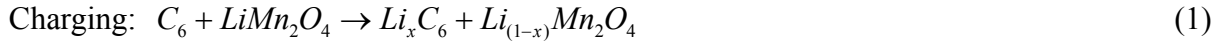
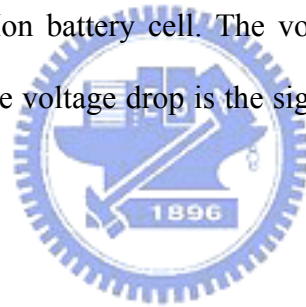


Fig. 2 The real structure of the Li-Ion battery



Under the charging condition, the battery is connected to the charger and the charging current flows from the anode to the cathode as equation (1) shown. When the battery is used as the source for the electrical device, the battery releases the energy stored in the cell and the discharging current flows backwards. The equation (2) shows the reaction during the discharging period. In general, the charging-terminated voltage of the Li-Ion battery is 4.2V and the discharging-terminated voltage is about 2.5V. To simplify the structure of the battery cell in the following discussion, the equivalent circuit of battery is drawn in Fig. 3. The battery cell includes the storage element C_{cell} and the equivalent resistance R_{cell} . R_{cell} is the parasitic resistance of the Li-Ion battery cell. The voltage of the V_{BATO} is the voltage drop across the storage cell C_{cell} . The voltage drop is the significant factor of the charger to charge the rechargeable battery.



Li-Ion Battery

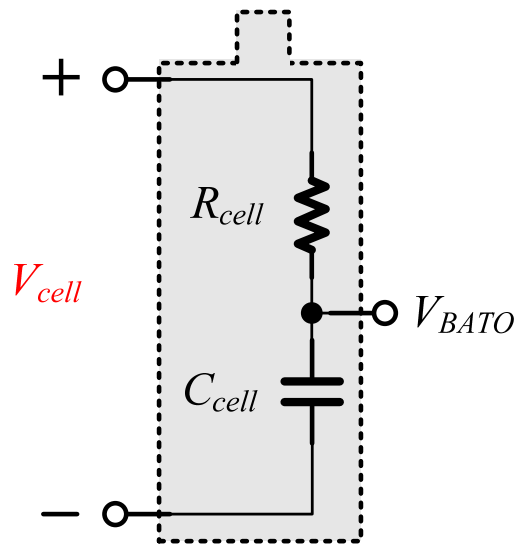


Fig. 3 The equivalent circuit of battery

1.3 The Package of the Charger

Fig. 4 shows the simple package of the charger. As illustrated in Fig. 4, the battery pack system includes the Li-Ion cell, the protection circuits, the external resistance, and the thermistor circuit [9].

In general, the protection circuit is composed of current limit, over-voltage limit, and under-voltage limit circuit. The life cycles of the battery is affected to the over-voltage and under-voltage, and the protection circuits of that could shut down the charger when the error signal is asserted. The over-current limitation circuit is used to control the charging current of the battery and protects the battery damaged from large current. As mentioned before, the physical component of the rechargeable battery is sensitive to the irregular operation, and the protection circuits could protect the battery from the above lethal injuries.

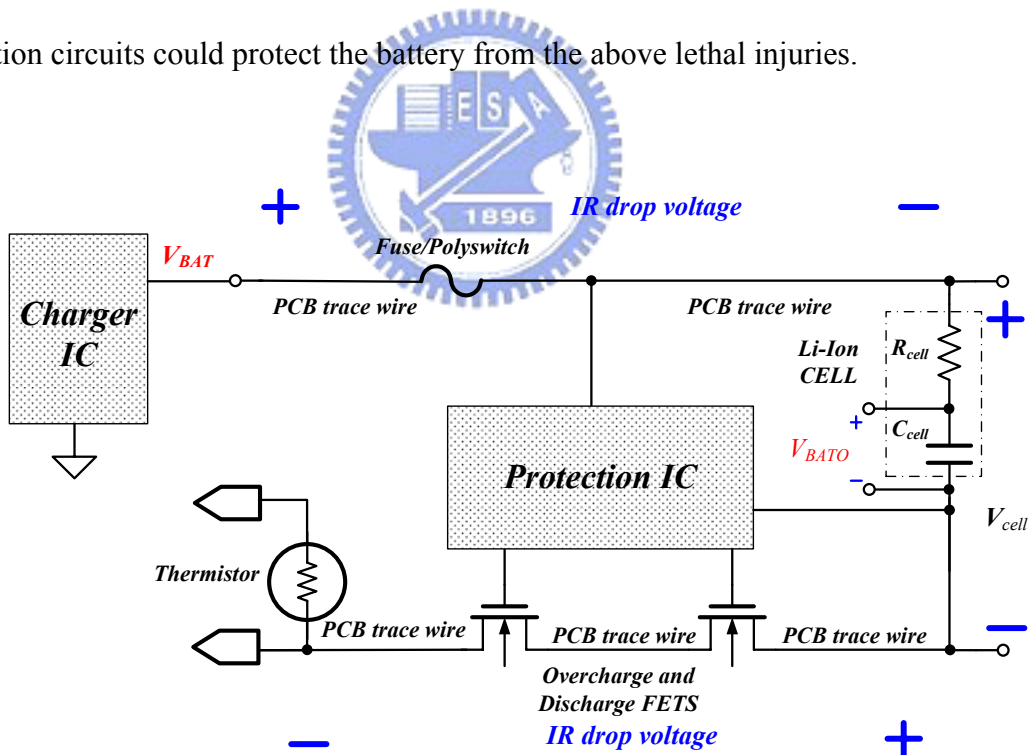


Fig. 4. The whole package of the charger IC and battery

The external resistance includes contacts, fuses, PCB trace wires, and cell resistances. The resistance could affect the charging process owing to the extra IR drop. When the charger charges the battery, the package of the charger and battery is easily overheated owing to the loss energy. Under the overheated condition, the electrolyte of the battery could be leak from the package. Even worse than that, the battery is under the risk of explosion in high temperature. The thermistor circuit is designed for detecting the temperature of the battery pack system to avoid overheating.

Fig. 5 is a conceptual schematic of the whole Li-Ion battery charging system. It shows the parasitic resistance of the battery pack system, the error amplifier regulates the voltage of the battery, the power MOS conducts the charging current, and the current source connected to the power supply.

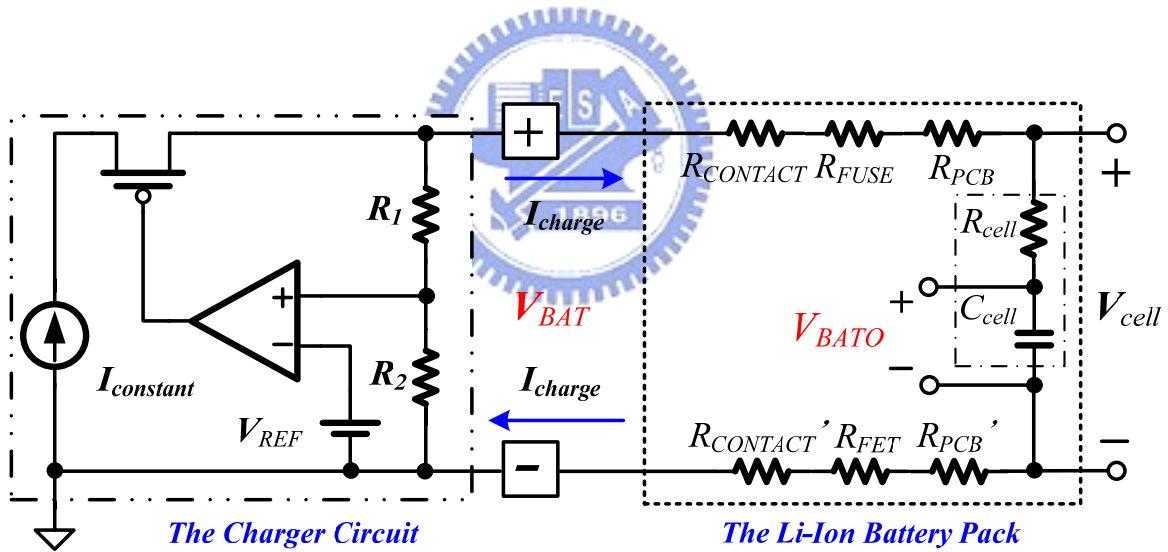


Fig. 5. The simplified circuits of the charger IC and battery

Due to the effect of the external resistance of all the extra elements, the voltage at the battery cell, V_{BATO} , is smaller than that at the output of the charger, V_{BAT} . Though the parasitic resistance of the external circuits is available, it results in the prediction error of the charger. The unwanted resistance consumes a part of the power charged to the cell and the IR-drop across the external resistance could leads the charger operates under the inappropriate mode.

1.4 Motivation

In order to prevent the battery from these injuries, there are many types of charger developed to charge the battery efficiently and safely. The most common charging method in present days is the CC-CV (Constant Current-Constant Voltage) method. First, the charger charges the battery in constant current to the specified voltage. Once the battery reaches the rated voltage, the charger enters the constant voltage mode and keeps the battery in stable voltage.

To protect the battery from being overcharging, the charging process needs to switch from CC stage to CV stage to charge the battery by a degrading current until the process is finished [10], [11]. However, the decision of the transition point from CC stage to CV stage is a stringent problem for the charger since the external resistance results the varied IR drop depends on the charging current. It may cause the operation mode switches between the two stages backwards and forwards. Besides, if the transition time is too early, the charging current drastically decreases and thereby the charging time of the Li-Ion battery is prolonged. Contrarily, if the transition time is too late, the large charging current may cause the battery voltage too high to damage the battery. In other words, the suitable transition point of the two stages affect not only the charging time but also the life cycle times of the battery.

In conventional design of the charger, the transition time of two stages is decided by the result of the comparator. The internal comparator detects the voltage of the battery and charges in larger current in CV stage. The charger switches the operation stage from the CC stage to the CV stage when the voltage at the output of the charger is raised to the default value. However, this specified voltage level of the Li-Ion battery pack varies with the charging current due to the IR drop across the external resistance. It is very hard to define the transition voltage level since the IR drop voltage varies with the value of the charging current and the external resistance, which depends on the structure of the Li-Ion battery pack.

Furthermore, the external resistance is also temperature-dependence. That is the value of the external resistance increases when the temperature of the Li-Ion battery pack increases. It is a hindrance to accurately predict the correct transition voltage [12], [13]. It implies that the usage of a comparator to determine the entrance point of CV stage is not adequate.

To reach the target of the smooth transition, this paper proposed the smooth control circuit (SCC) to realize that. The charger controls the charging process in current mode to avoid the vibration of the battery voltage. The other issue, early entrance to the CV stage, is solved by the built-in resistance compensator (BRC). The novel technique could modify the prediction error and gain the better efficiency.



Chapter 2

The Basic Concept of the Conventional Charger and the Prior CC-CV Charger

From the previous discussion, the charger plays an important role in the use of battery. The defective charger could prolong the charging time of the charging process and reduce the life cycles of the rechargeable battery. The charger concerns not only the battery cell but also the battery pack system. To enhance the performance of the charger and not to damage the battery back, there are many types of charger developed.

In this Chapter, the roughly introduction of the charger will be illustrated. The chapter is divided into three sections. Section 2.1 introduces the charging method of the Ni-MH, Ni-Cd, and Li-Ion charger. For the different types of rechargeable battery, there are many types of charging method developed to meet the characteristics. Section 2.2 introduces the properties of the conventional Li-Ion battery charger and section 2.3 introduces the prior art to solve the problems in section 2.2 and the proposed technique of smooth control circuit (SCC) and built-in resistance compensator (BRC).

2.1 The Concept of the Charging Method for Ni-based battery and Li-based battery

This section introduces the main charging method of the Ni-MH, Ni-Cd, and the Li-Ion rechargeable battery. For different types of rechargeable battery, there are many charging methods to charge the battery for better performance. Section 2.1.1 introduces the voltage controlled charging method of Ni-MH and Ni-Cd battery. Section 2.1.2 introduces the constant current to constant voltage (CC-CV) charging method of Li-Ion battery.

2.1.1 The Voltage-Controlled Charging Method for Ni-MH, Ni-Cd battery



For the Ni-MH, Ni-Cd battery, there are many charging method to charge the battery, ex: timer-controlled method, voltage-controlled method. However, the initial state of each battery is different and it makes the charging time different. That is, the timer controlled method is not appropriate to the general batteries. The voltage-controlled method includes max-voltage control, zero delta-voltage control, and negative delta-voltage control. Among these methods, the negative delta-voltage is the chief application to the Ni-Cd battery and the zero delta-voltage control charging method for Ni-MH battery. The charging waveform is shown in Fig. 6.

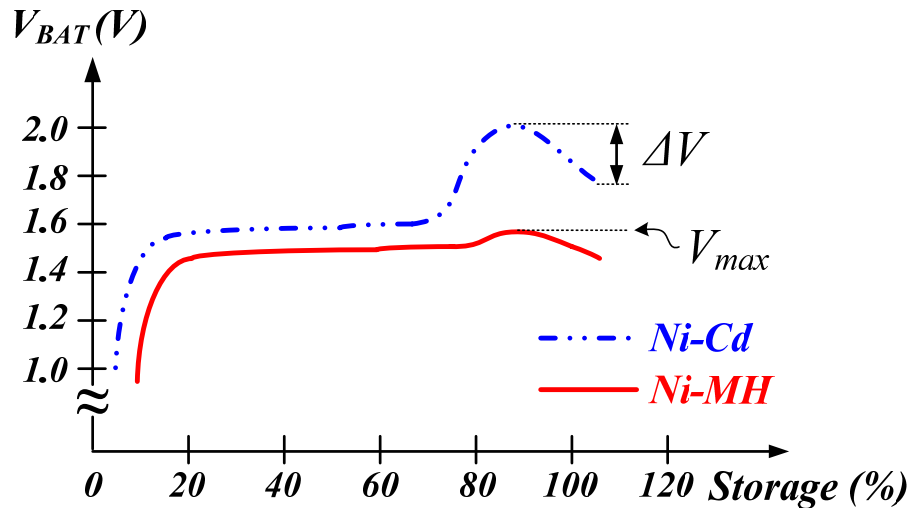


Fig. 6. The charging waveform of the Ni-MH and Ni-Cd battery

Compared with the Ni-MH battery, the negative voltage drop of V_{BAT} of Ni-Cd battery is larger than that of Ni-MH battery. It implies that the detection of negative delta-voltage method is appropriate to Ni-Cd battery. When the Ni-MH battery is charged in trickle current, the voltage drop of V_{BAT} is smaller and even does not exist. Therefore the zero delta-voltage control method is applied to the Ni-MH battery.

When the battery is connected to the charger, the charger charges the battery in constant current. At the beginning of the charging process, the resistance of the electrolyte affects the charging speed of the battery. The voltage of the battery rises in high speed. During the charging period, the resistance reduces and the charging speed is slow down. When the energy is nearly full-charged to the battery, the gas bubbles of the electrolyte increase and the resistance is getting higher. It makes the voltage of V_{BAT} reach the max voltage promptly. For the Ni-Cd battery, when the battery is charged to the rated level, the voltage of the battery will drop the value of ΔV . The charger detects the negative delta-voltage and terminates the charging process. For the Ni-MH battery, the charger detects the max voltage and terminates immediately.

2.1.2 The Constant Current to Constant Voltage Charging

Method for Li-Ion Battery

Generally speaking, the charging process of Li-Ion battery charger is divided into three charging stages, i.e. trickle-current stage (TC), constant-current stage (CC), and constant-voltage stage (CV) as listed in TABLE III. At the beginning of the charging process, the charger detects the initial voltage of the battery V_{BAT} . If voltage V_{BAT} is smaller than the specified voltage V_{REF} (normally 2.5V), the charger starts from the TC stage with a trickle charging current for avoiding the damage due to large charging current on the battery. That is the pre-charge stage. Once the value of V_{BAT} is larger than that of V_{REF} , the charging process is switched from TC stage to the CC stage. The charger operates at the CC stage with a constant and large driving current until the value of V_{BAT} exceeds that of V_{FULL} (normally 4.2V), which is a predefined transition voltage, and thereby entering the CV stage. The charger then charges the cell in degrading current to the full capacity until the process stops.

There are two methods to terminate the charging process. One is monitoring the minimum charging current at the CV stage. The charger completes the charging process when the charging current is decreased to the specified range. The other one to finish the charging process is based on the maximum charging time [14].

The so-called fast-speed charger sold in the market is designed to terminate the charging process when the voltage of V_{BAT} is charged to rated voltage, 4.2V. It implies that the charger does not enter the CV stage and the cell is not full charged. In other words, the using time of the fast-speed charged battery is lesser than the normal charged battery.

TABLE III

THE THREE OPERATING MODE OF THE CONVENTIONAL CHARGER

V_{BAT}	<i>Charging Process</i>	<i>Charging State</i>
$< V_{REF}$	● Trickle Current (TC)	● Low charging current
$> V_{REF}, < V_{FULL}$	● Constant Current (CC)	● Larger, well-regulated current
$> V_{FULL}$	● Constant Voltage (CV)	● Constant Voltage ● Low current

The simplified diagram of Li-Ion battery charger is shown in Fig. 7. The basic structure of the charger includes the three error amplifiers CA, VA, and MA. The transistor, M_{CS} , is the current sensing circuit of the powerMOS, M_P . R_1, R_2 is the feedback resistor to divide the voltage of V_{BAT} and used to decide the operating mode of the charger.

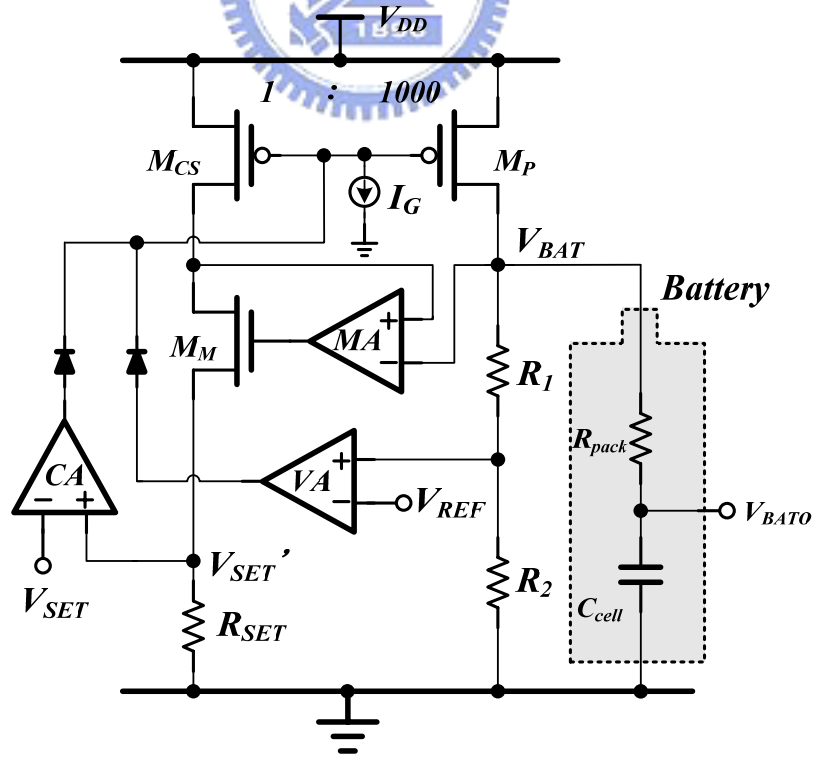


Fig. 7. The conceptual structure of the basic charger circuit.

Referring to Fig. 5, the resistance R_{pack} is defined as:

$$R_{CONTACT} + R_{FUSE} + R_{PCB} + R_{CONTACT}' + R_{FET} + R_{PCB}' + R_{cell} = R_{pack} \quad (3)$$

When the charger operates at the TC stage and CC stage, the battery is charged with a constant current that is decided by the values of the V_{SET} and R_{SET} . That is the closed-loop is established by the amplifiers, MA and CA [15]. Thus, the value of V_{SET}' is close to that of V_{SET} through the virtual short of the CA. Besides, the value of V_{SET} at the TC stage is set relatively smaller than that at the CC stage. The charging current at the TC stage is smaller than that at the CC stage to pre-charge the cell. The trickle current at the TC stage protects the battery from being damaged under low battery voltage condition. When the battery is charged to an adequate voltage of 2.5V, the charging process is switched to the CC stage automatically. Once the charging process enters the CC stage, the IR drop voltage across the external resistance immediately becomes larger than transition level, 2.5V since to the charging current at the CC stage is larger than that at the TC stage. The charging process enters into the CC stage and never comes back to the TC stage again if the charging process continues and the voltage of the cell does drops below 2.5V.

Similarly, the charging current at the CC stage is larger than that at CV stage. It means much energy is rapidly stored in battery during the CC stage. When the battery voltage reaches the rated voltage V_{FULL} , 4.2V, the operating process is switched to CV stage. However, it is too early to enter the CV stage since the battery voltage is the summation of the voltage at battery cell (V_{BATO}) and the IR-drop voltage. At the CV stage, the operation amplifier VA acts as a linear regulator [16], [17] and generating a gradually decreasing current, which may minimize the possibility that the charger is switched between the CC and CV stages.

2.2 The Properties of the Conventional Charger

As mentioned before, the parasitic resistance of the external component results in the operation error in the charging process. This section introduces the defect of the conventional charger. In Chapter 2.2.1, the iteration between CC and CV stage is illustrated. And the drawback of the early entrance to CV stage is introduced in Chapter 2.2.2.

2.2.1 The Unstable Transition of CC to CV Stage

The trickle current stage charges the battery when the battery is under the low voltage. The operation of the TC stage ensures that the battery exceeds the adequate voltage level and charges it in larger current in CC stage. In initial method of charging, the charger charges the battery in constant voltage or constant current [18]. If the battery is charged in constant voltage, the time of the charging is limited to the supply voltage. The low supply voltage prolongs the charging progress and the high supply voltage may damage the rechargeable battery. In the meanwhile, the constant current method could results in the same problem. That is the reason that the TC-CC-CV charging method is the main application in the charger nowadays.

However, there is a latent problem exists in the transition point of the CC to CV stage. When the charger is switched from the CC stage to CV stage, the charging current of the charger starts to decrease and the disappearance of the large IR-drop voltage at the CV stage still causes the charger having an unstable condition as conceptually illustrated in Fig. 8. The use of the comparator, which compares the voltage at the battery pack and the predefined rated voltage V_{FULL} , causes the early entrance of the CV stage.

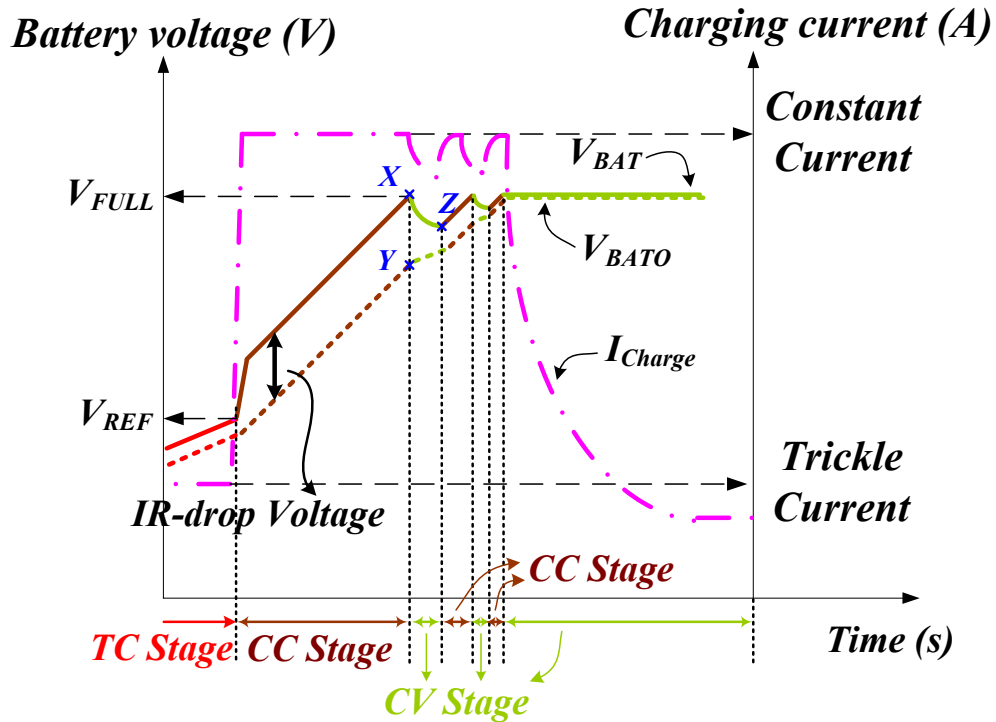
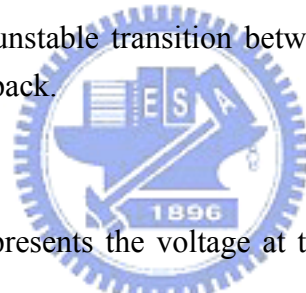


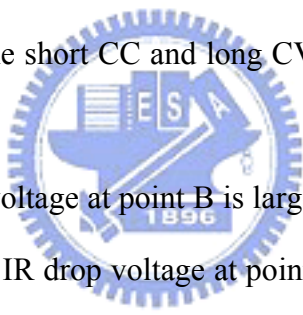
Fig. 8. The waveform of the unstable transition between the CC and CV stages due to the IR-drop voltage of the battery pack.



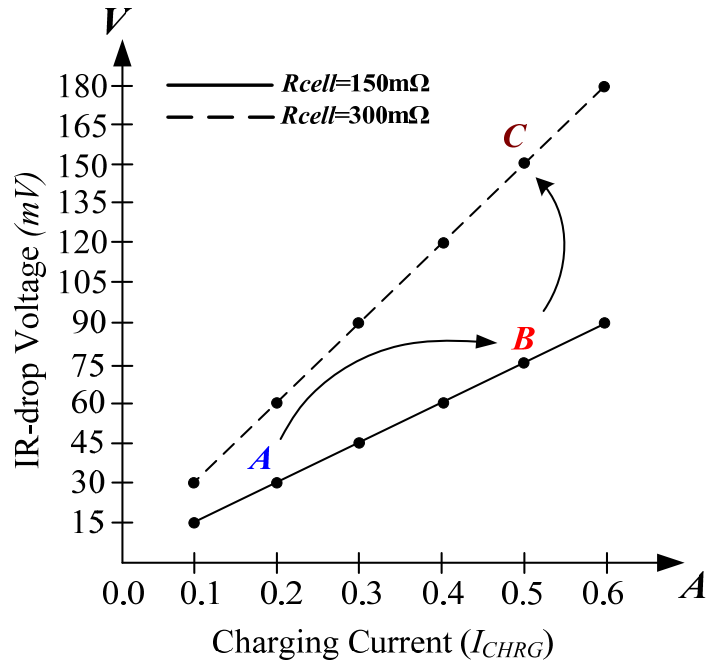
In Fig. 8, the point X represents the voltage at the battery pack, V_{BAT} and the point Y stands for the voltage at the battery cell, V_{BATO} . The output of the comparator can decide transition point of the charging stage but can't account for the effect of the external resistance when the predefined rated voltage V_{FULL} is set to 4.2V. Furthermore, due to the gradually decreasing charging current for avoiding overcharging, the voltage at the battery pack (V_{BAT}) will become smaller than the predefined rated voltage V_{FULL} . At this time, the charging process comes back to the CC stage once again since the voltage at the battery pack is decreased to point Z in Fig. 8. The iteration will continue many times until the voltage at the battery cell is close to the rated voltage V_{FULL} . There are two disadvantages existed in the above charger design. One is the longer charging time due to the early entrance of the CV stage. The other one is the unstable transition between the two stages.

2.2.2 The Short Duration of the CC Stage

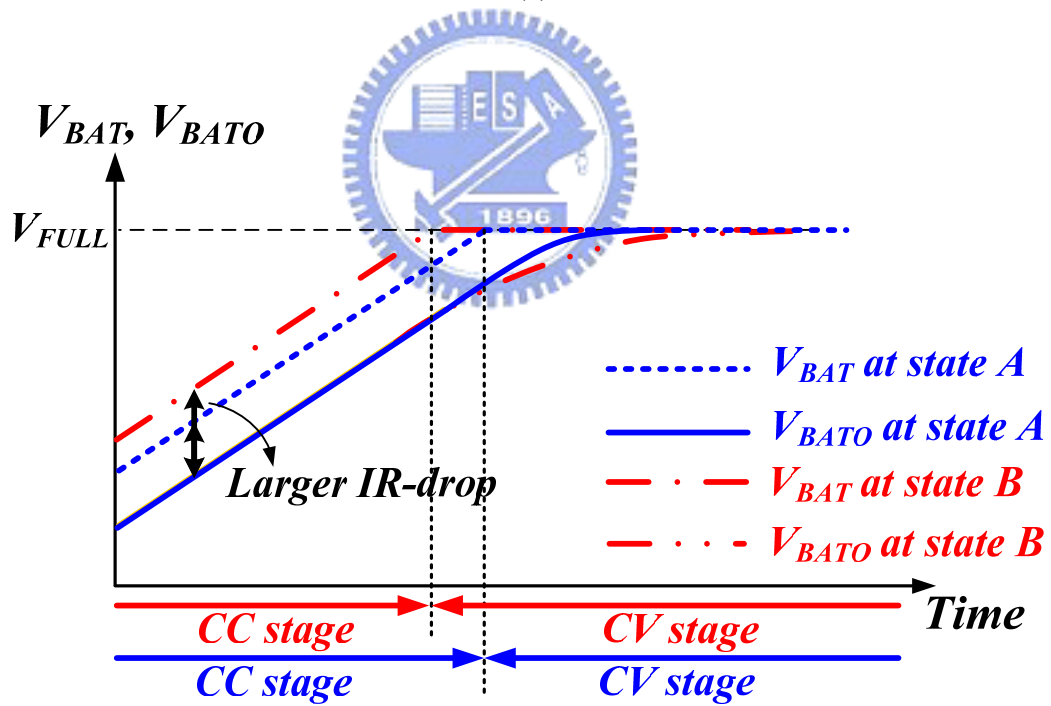
Owing to the effect of the external resistance, the early entrance of the CV stage could prolong the whole charging process. A large charging current causes large IR-drop voltage across the external resistance in the Li-Ion battery pack system. It makes the charger circuit detects the transition point of the CC stage to CV stage more early than that with a small charging current. The IR-drop voltage is added to the voltage V_{BATO} at battery cell before the voltage V_{BATO} is fully charged to the rated voltage level. It indicates that the IR-drop voltage affects the optimum transition point from the CC stage to the CV stage. In other words, it takes a long time to charge the battery to the rated voltage at the CV stage when using a large charging current in CC stage. That is a larger charging current at the CC stage can't reduce the charging time because of the short CC and long CV periods. Finally, the total charging is prolonged.



In Fig. 9 (a), the IR-drop voltage at point B is larger than that at point A due to the larger charging current. Besides, the IR drop voltage at point C is larger than that at point B due to the larger external resistance. Briefly speaking, the IR-drop voltage depends on the product of the charging current and the external resistance. The charging timing diagrams of points A and B in Fig. 9 (a) are illustrated in Fig. 9 (b). Obviously, the charging time is prolonged when the charging current is large due to the short CC period. That is the duration of CC stage plays an essential role in the evaluation of the charging time. The existing charger circuits suffer from the drawback of inaccuracy of the transition point from the CC to CV stage. In order to shorten the charging time, the compensation of the IR-drop voltage is a critical problem to be solved.



(a)



(b)

Fig. 9. The IR-drop voltage under the different charging current and R_{pack} . (a) The IR-drop voltage is affected by the product of the charging current and the external resistance. (b) The charging timing diagrams of points A and B in (a).

2.3 The Prior Art and the Proposed Method

Since the unstable transition and the early-entrance to CV stage are two critical problems to be solved urgently in charging process, this section provides the solution and proposes the new circuit. Section 2.3.1 described the analogy method to control the charging operating mode, and the section 2.3.2 is the proposed technique to solve the early entrance of the rechargeable battery charger.

2.3.1 The Analogy Transition Method to CC Stage and CV

Stage

In the proposed charger circuit, the decision of the charging transition is an analogy method in order to have a smooth transition between the CC and CV stages. The analogy-control method is achieved by the smooth control circuit (SCC). Referring to Fig. 10, the SCC contains the current mirror M_1 , M_2 , the pass transistor M_{CA} , and the current source I_G . The current loop is controlled by the amplifiers, MA and CA while the voltage loop is controlled by the amplifier VA. In conventional digital control method, the transition of the CC-CV stage is decided by the internal voltage comparator. However, the analogy method utilizes the push-pull technique to control the voltage level of the gate of the powerMOS, M_p .

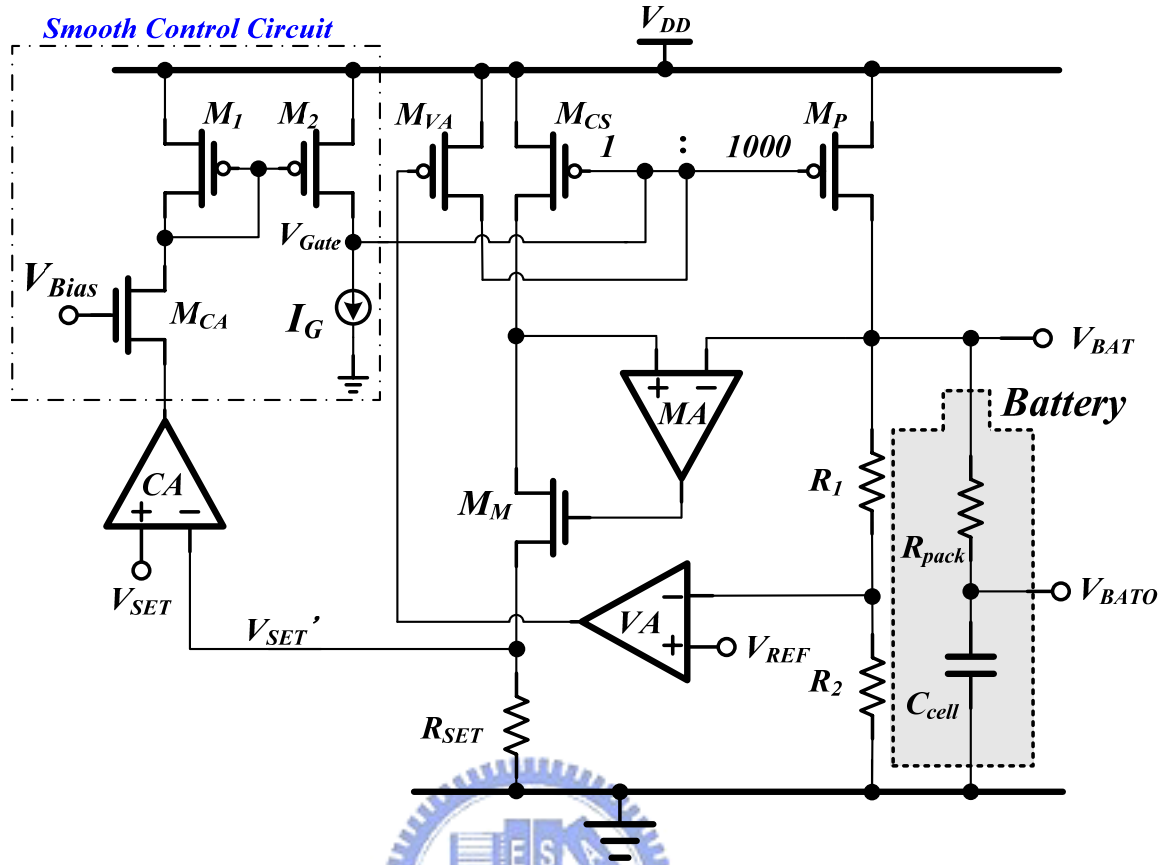


Fig. 10. The simplified diagram of the charger based on the analogy method.

At the beginning of the charging process, the voltage at the battery pack is low and causes the output of the amplifier VA high enough to turn off the transistor M_{VA} . Thus, the voltage loop has no effect on the charging current. That is the charging current, which is equal to V_{SET}/R_{SET} , is controlled by the current loop. Once the voltage V_{BAT} is approaching to the rated V_{FULL} , the output voltage of the amplifier VA is low enough to turn on the transistor M_{VA} to overcome the constant current I_G . Therefore, the voltage at the gate of the power MOSFET M_P is also raised to a voltage level to decrease the current flowing through the transistor M_{CS} . The voltage V_{SET}' is decreased to cause the output of the amplifier CA high enough to turn off the pass transistor, M_{CA} . Therefore, there is no current flow through the current mirror M_1, M_2 , and the current loop is turned off automatically. Then, the charging process is smoothly

switched from the CC stage to the CV stage by SCC. At the CV stage, the operation amplifier VA takes the control of the charger and the charger acts as a linear regulator. The charger keeps the battery at a regulated voltage V_{FULL} until the charging process is terminated.

2.3.2 The Solution to the Early Entrance of the CV Stage

In the attempt to minimize the error due to the external resistance in the Li-Ion battery pack system, the commercial charger circuits uses the external compensation resistors to compensate the IR-drop voltage [19]. The major disadvantage is that the module of the charger is too large to be compact for portable devices. Besides, the compensation resistors can't be adapted to the variations of the external resistance in the Li-Ion battery pack system due to thermal effect. Therefore, the built-in resistance compensator is proposed in this paper to make the module of the charger be compact and prolong the period of the CC stage.

Owing to the longer duration at the CC stage and the shorter duration at CV stage, the Li-Ion cell can be charged to more closely approach to the rated voltage even that the external resistance in the Li-Ion battery pack system varies with thermal effect. The behavior of the proposed charger with the BRC technique in presence of shorter duration of the CV stage can effectively shorten the charging time of the battery to achieve the fast charging technique.

Chapter 3

The Circuit Implementation of BRC and SCC Technique and Simulation Result

When the voltage V_{BAT} of the battery pack system reaches the rated voltage V_{FULL} , the voltage V_{BATO} at the Li-Ion cell is smaller than that. Because the external resistance results in an IR-drop voltage across the external resistance, the energy of battery cell is not fully charged. The IR-drop voltage prolongs the period of the CV stage and thus increases the charging time to storing sufficient energy on the Li-Ion battery cell. The IR-drop voltage is the product of the external resistance R_{pack} and the charging current. Referring to Fig. 9, the insufficient energy due to the IR-drop voltage is needed to be compensated during the CV stage. Particularly, in case of charging the battery with a large current like the movement from point A to point B, the IR-drop voltage is larger and the charging time is also prolonged due to the longer CV period.

Even that the external resistance can be estimated and compensated by external method, the value of the external resistance still varies with temperature. The increasing external resistance also increases the IR-drop voltage, and thereby increasing the charging time. The movement from point B to C can reveal this scenario. It means that a fixed compensation method for the external resistance is still inaccurate. In other words, the compensation is needed to be done before the transition from the CC stage to the CV stage. Certainly, the compensation method also needs to tolerate the variation of temperature

3.1 The Implementation and Simulation of SCC

(Smooth Control Circuit) Technique

As Fig. 10 shown, the smooth control circuit contains the current mirror M_1 , M_2 , the pass transistor M_{CA} , and the current source I_G . The main advantage of the current loop control is that there would be no voltage vibration. During the TC and CC stage, the charging current is controlled by the amplifier CA. The gate voltage of powerMOS M_P , is decided by the output current of M_2 . The amplifier VA takes control when the voltage of V_{BAT} reaches the rated voltage and the charger enters the CV stage. The transistor M_{VA} then outputs the current to raise the gate voltage of M_P . The voltage variation of the V_{Gate} during the transition from CC to CV stage is shown in Fig. 11.

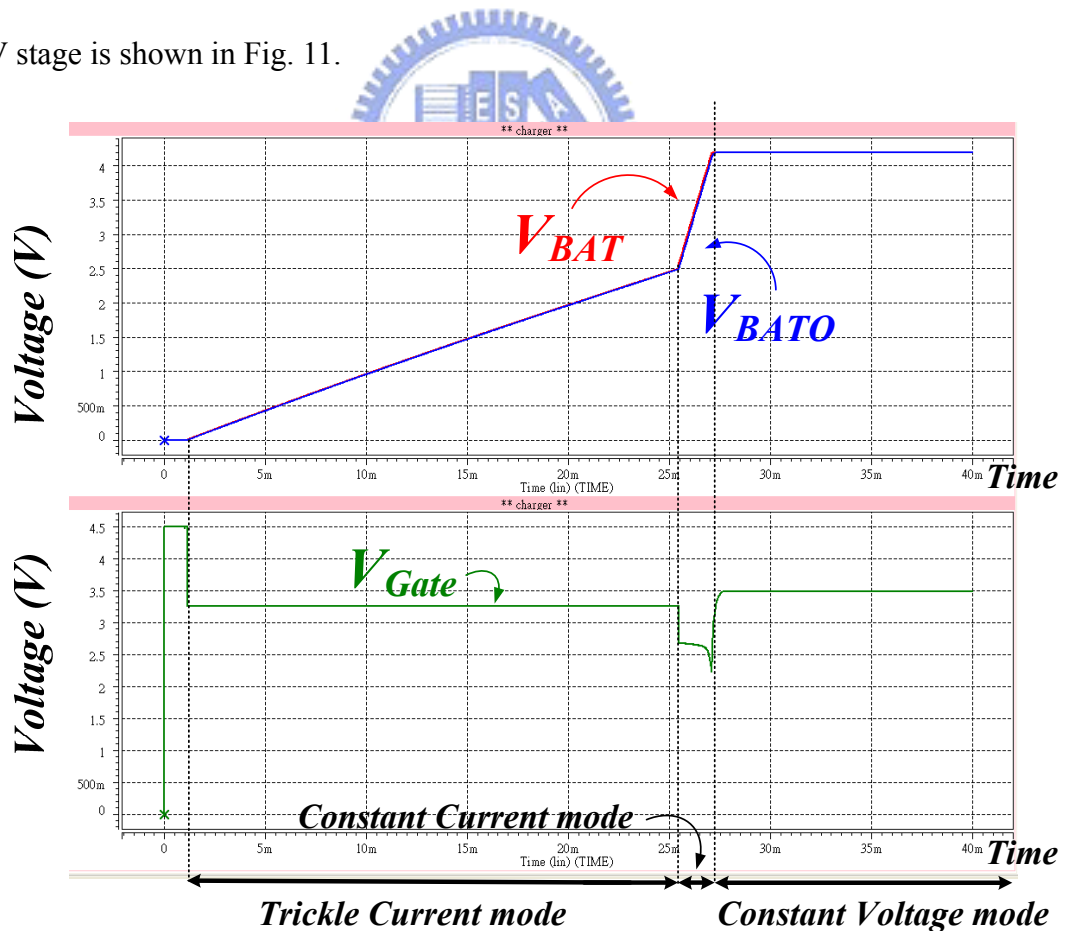


Fig. 11. The improved waveform of the charger with SCC technique.

Fig. 11 shows that the voltage of V_{Gate} changes smoothly to control the charging current of the three stages. When the charger is working in the CC stage, the voltage of V_{Gate} is lower than that of TC stage to conduct the larger charging current. Once the battery is almost fully-charged, the gate level is getting lower to conduct the same constant current owing to the rise of V_{BAT} . After the battery reaches the rated voltage, the amplifier, VA starts to control the charger and regulate the voltage of V_{BAT} in 4.2V. It implies that the V_{Gate} must be lifted to complete the regulation loop.

The transition from the current loop to voltage loop is smoothly referred to Fig. 11. As Fig. 12 shown, the gate level is controlled by the current source of transistor M_2 and M_{VA} . The current of amplifier, VA is getting larger to takes control of the charger. Once the current is supplied by the VA completely, the amplifier, CA does not affect the charger and the current loop is removed.

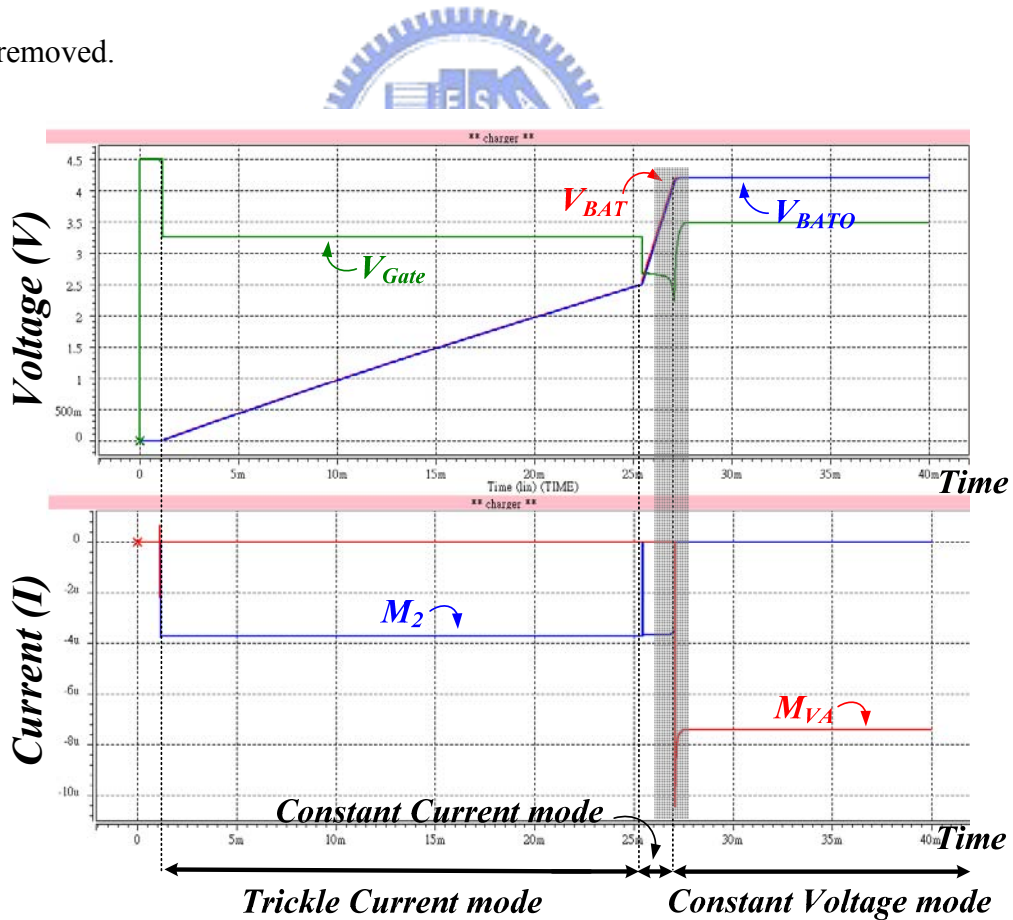


Fig. 12. The drain current of the transistors M_{VA} and M_2

3.2 The Circuit Concept, Implementation, and Simulation of BRC Technique

Chapter 3.2 introduces the basic structure of the BRC technique. The chapter is divided into five sections. Section 3.2.1 introduces the idea of the BRC technique. Section 3.2.2 is the formulas derivation of the technique. Section 3.2.3 illustrates the simple structure and the working principles of the charger with BRC technique. Section 3.2.4 introduces the detection of the external resistance and section 3.2.5 is the introduction of the reference shift circuit.

3.2.1 The Concept of BRC Technique

To solve the problem, a BRC technique is applied in the charging process to improve the performance. As depicted in Fig. 9, since the difference voltage between the voltage V_{BATO} at the Li-Ion cell and the voltage of the battery V_{BAT} is the IR-drop voltage, it implies that the reference voltage can be shifted to a higher voltage level and re-define the final voltage level of V_{BAT} . The shift reference voltage is defined as V_{REFC} and the re-defined voltage level of V_{BAT} is V_{BATC} . As a result, the voltage V_{BATO} at the Li-Ion cell can be closely approached to V_{FULL} at the end of the CC stage owing to the higher reference voltage.

Fig. 13 shows the comparison of the charging waveform with a higher V_{REFC} and that with an uncompensated V_{REF} . Obviously, the period of the original CC stage is extended to CC' stage after using the BRC technique.

In order to compensate the IR-drop voltage, a new reference voltage V_{REFC} , which is the summation of the increment voltage V_{INC} and the original reference voltage V_{REF} , is introduced. The increment voltage V_{INC} is defined as [20]:

$$V_{INC} = (V_{BATO} - V_{BAT}) \times \frac{R_2}{R_1 + R_2} = IR_{drop} \times \frac{R_2}{R_1 + R_2} \quad (4)$$

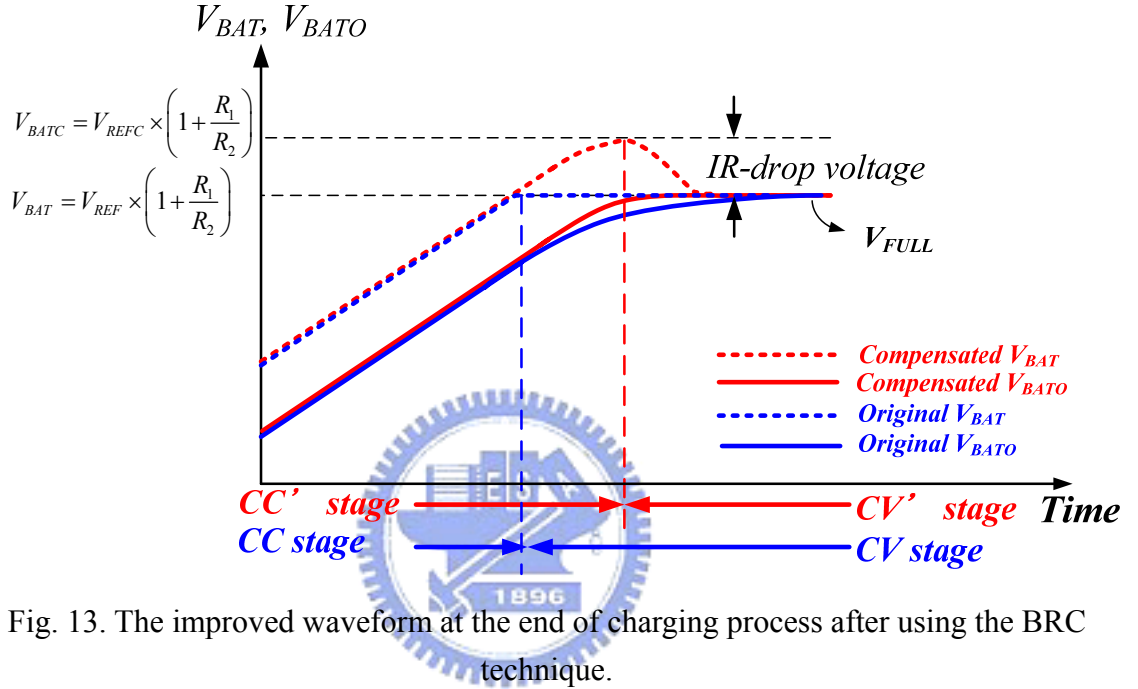


Fig. 13. The improved waveform at the end of charging process after using the BRC technique.

Thus, the voltage of the battery pack system is charged to a higher voltage level at the end of the CC stage. The Li-Ion battery cell can be stored much more energy at the CC' stage for a longer period than that at the CC stage based on the original design. Once the charging process enters the CV stage, the reference voltage at the CV stage is decreased back to its original value gradually. Thus, the battery can be charged to the designated voltage V_{FULL} when the charging process is ended. By using the dynamic reference voltage method, not only the charging time can be decreased but also the overcharging problem will not occur in the charging process.

3.2.2 The Estimation of the External Resistance at the CC

Stage

In order to determine the value of the variable external resistance, it is important to find out a method to accurately estimate the value. Before the charging process is switched to the CV stage, the voltage V_{BATO} at the Li-Ion cell is smaller than the specified voltage V_{FULL} due to the IR-drop voltage. Based on the fact that charger charges the battery cell tardily when the battery voltage V_{BAT} is close to 4.2V, the voltage V_{BATO} of the Li-ion cell can viewed as a constant during a short test time.

At the beginning of the estimation, the charging current is changed from I_{CHRG1} to I_{CHRG2} . It causes a voltage difference at the battery voltage V_{BAT} owing to the voltage drop across the external resistance R_{pack} as depicted in Fig. 9. At the Li-Ion battery pack, the two battery voltages V_1 and V_2 can be written as (5) and (6) according to the two different charging current I_{CHRG1} and I_{CHRG2} , respectively.

$$V_1 = (I_{CHRG1} \times R_{pack}) + V_{BATO1} \quad (5)$$

$$V_2 = (I_{CHRG2} \times R_{pack}) + V_{BATO2} \quad (5)$$

According to the previous assumption that V_{BATO1} and V_{BATO2} are equal to each other within a small charging time, the external resistance R_{pack} can be estimated by (7).

$$R_{pack} \approx \frac{V_1 - V_2}{I_{CHRG1} - I_{CHRG2}}, \text{ assuming that } V_{BATO1} \approx V_{BATO2} \quad (6)$$

Therefore, if the three parameters I_{CHRG1} , I_{CHRG2} , and V_1 are pre-defined, the value of R_{pack} can be determined by the estimated value of the battery voltage V_2 . The BRC technique provides the internal detection method to acquire the voltage, V_2 .

3.2.3 The Proposed Architecture of the Charger with the BRC Technique

The proposed architecture of the charger with the BRC technique is shown in Fig. 14. The compensation circuit is composed of the external resistance detector, the reference voltage switch circuit, and the reference shift circuit.

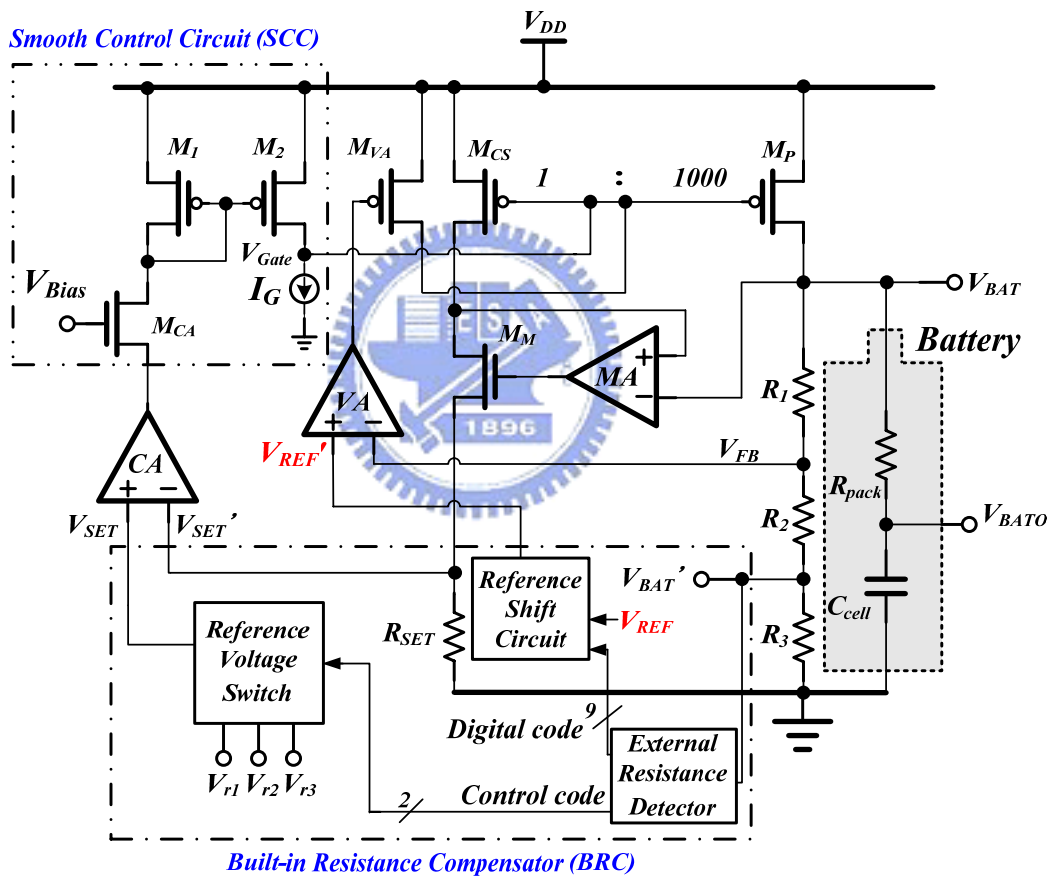


Fig. 14. The proposed fast-charging charger with the external resistance estimation.

The external resistance detector is used to determine the value the external resistance of the Li-Ion battery pack. The feedback voltage V_{FB} is equal to (8). However, the input voltage V_{BAT}' is designed as (9) to meet the requirement of the headroom of the detector circuit and the supply voltage. The outputs of the external resistance detector contain two parts. One part

is the 9-bit digital code to determine the new reference voltage. The other part is the 2-bit control code to determine the status of the estimation. The 2-bit control code decides the output voltage of the reference voltage switch during the estimation period. Finally, according to the 9-bit digital code, the reference shift circuit outputs a compensated reference voltage, V_{REFC} to extend the period of the CC stage.

$$V_{FB} = V_{BAT} \cdot \frac{R_2 + R_3}{R_1 + R_2 + R_3} \quad (7)$$

$$V_{BAT}' = V_{FB} \cdot \frac{R_3}{R_2 + R_3} = V_{BAT} \cdot \frac{R_3}{R_1 + R_2 + R_3} \quad (8)$$

For the reference voltage switch circuit, the input voltages V_{r1} and V_{r3} are used to decide the charging current at TC stage and CC stage, respectively. That is the voltage V_{SET} is set to V_{r1} (or V_{r3}) at the TC (or CC) stage under normal charging process. Undoubtedly, the value of V_{r3} is larger than that of V_{r1} for ensuring a large charging current at the CC stage. Here, a new rated voltage V_{r2} is used to decide another charging current at the CC stage for the external resistance estimation. Thus, the values of the two constant charging currents I_{CHRG1} and I_{CHRG2} can be defined as (10) and (11), respectively.

$$I_{CHRG1} = \frac{V_{r3}}{R_{SET}} \quad (9)$$

$$I_{CHRG2} = \frac{V_{r2}}{R_{SET}} \quad (10)$$

The value of the voltage V_{SET} is maintained at the value of V_{r3} at the CC stage for conventional design. However, for the proposed charger, the value of V_{SET} is changed from V_{r3} to V_{r2} at time (t_2) and set back to V_{r3} at time (t_3) at the end of CC stage during the estimation of the external resistance. The variation of the value of the voltage V_{SET} will cause a variation of the charging current. Consequently, the voltage at the Li-Ion battery pack also will be affected due to the different IR-drop voltages. That is the battery voltage V_{BAT} changes

from V_1 to V_2 as depicted in Fig. 15. Referring to equation (7), the voltage of V_1 is pre-decided and the voltage of V_2 is needed to be estimated. In order to accurately detect the variable external resistance in the Li-Ion battery pack, the predefined detection point is designed at $V_{BAT}=V_1=4V$. In the proposed charger, the value of the R_1+R_2 is equal to the value of R_3 to sense half the value of V_{BAT} . According to (9), the voltages V_1 and V_2 are redefined as V_1' and V_2' , respectively. That is the values of V_1' and V_2' are half of that of V_1 and V_2 . In the meanwhile, the value of V_1' is equal to 2V.

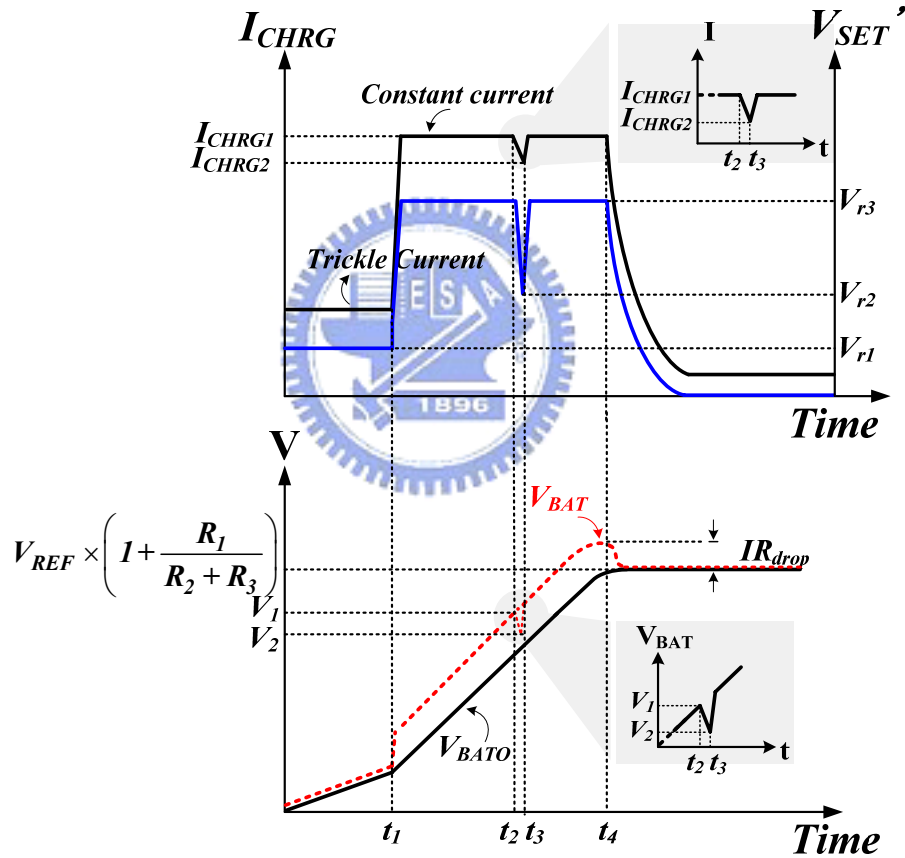


Fig. 15. The waveform of battery voltage during detecting period.

The simulation of the waveform of the detection period is shown in Fig. 16 and Fig. 17 respectively under different condition. Fig. 16 shows the voltage variation of V_{BATO} during the detection period when the external resistance is 150mΩ. The charging current is switched from I_{CHRG1} (500mA) to I_{CHRG2} (300mA), and the corresponding V_{SET}' is from 1.5V to 0.9V.

Referring to equation (12), the voltage drop of V_{BATO} when the external resistance is $150m\Omega$ is:

$$V_{drop150} = (I_{CHRG1} - I_{CHRG2}) \times R_{pack150} = (500mA - 300mA) \times 150m\Omega = 30mV \quad (11)$$

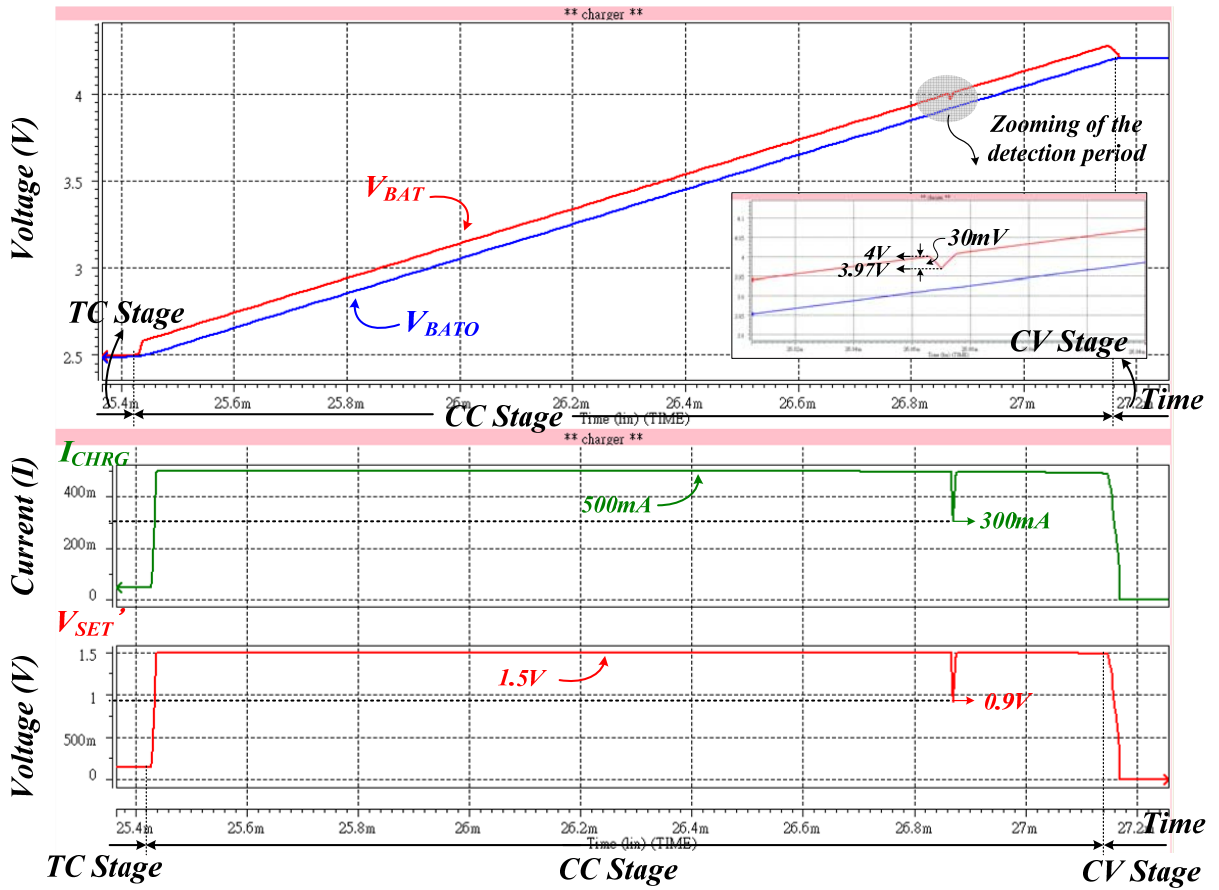


Fig. 16. The waveform of V_{BAT} , V_{BATO} , V_{SET} , and I_{CHRG} during the detection period, $R_{pack}=150m\Omega$

The voltage drop of V_{BATO} when the external resistance is $300m\Omega$ is:

$$V_{drop300} = (I_{CHRG1} - I_{CHRG2}) \times R_{pack300} = (500mA - 300mA) \times 300m\Omega = 60mV \quad (12)$$

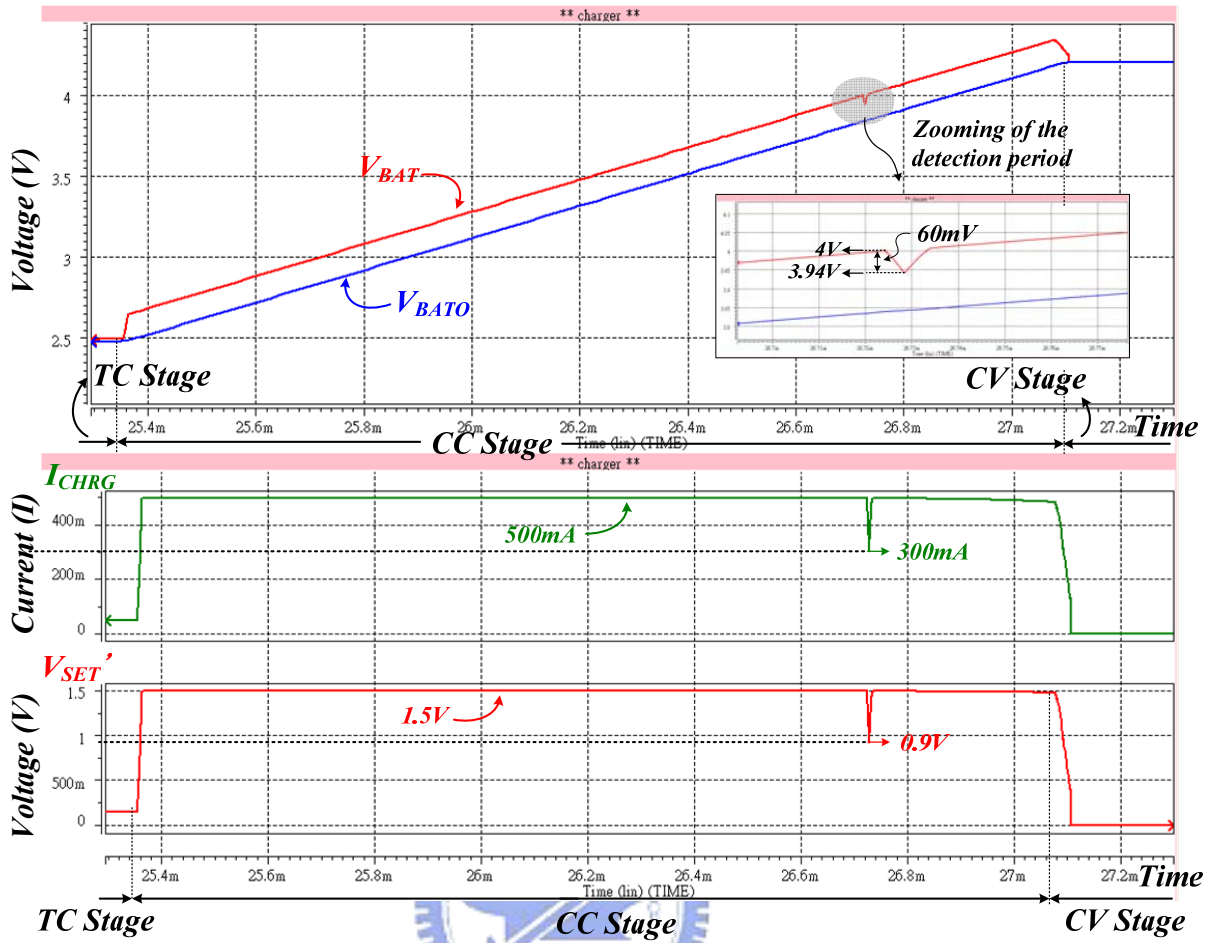


Fig. 17. The waveform of V_{BAT} , V_{BATO} , V_{SET}' , and I_{CHRG} during the detection period, $R_{pack}=300m\Omega$

The Fig. 16 and Fig. 17 show that the detection period starts when the voltage of V_{BAT} reaches 4V. The value is the pre-defined voltage and the charger is closing to the transition point from CC to CV stage at this period to acquire the more accurate external resistance. Obviously, the detection period is able to neglect to the whole charging process. The charging process would not be effect with the proposed technique.

3.2.4 The Proposed External Resistance Detector and the Reference Voltage Switch Circuit

Fig. 18 shows the whole detailed circuit of the external resistance detector. The value of the voltage V_{BAT} is V_1' at time t_2 when the control signal Φ_1 turns from low to high and the value of the voltage V_{BAT} reaches 4V. Certainly, the value of the voltage V_{SET}' is V_{r3} for defining the charging current I_{CHRG1} . By using a sample-and-hold (S/H) circuit [21], the voltage V_1' is stored on the capacitor C_{SH1} . When the value of the voltage V_{SET}' reaches V_{r2} for defining the charging current I_{CHRG2} , the control signal Φ_2 turns from high to low and the estimated value of V_2' at time t_3 is stored on the capacitor C_{SH2} . The two values V_1' and V_2' are sent to the differential inputs of the G_m amplifier, which has the transconductance of $2/R_{VI}$, as shown in Fig. 18 (a) [22], [23]. The charge injection and clock feed-through of the S/H circuits can be ignored owing to the differential operation. Thus, the accuracy is not affected during the detection period. The value of the output current I_{DROP} is proportional to the difference of the two voltages V_1' and V_2' . The expression of the current I_{DROP} is shown as (14).

$$I_{DROP} = G_m \cdot (V_1' - V_2') = \frac{2}{R_{VI}} \cdot (V_1' - V_2') = \frac{2}{R_{VI}} \cdot 2 \times (V_1 - V_2) = \frac{2}{R_{VI}} \cdot 2IR_{drop} \propto IR_{drop} \quad (13)$$

As illustrated in Fig. 18 (a), the current I_{DROP} is mirrored to bias the delay-line circuit in Fig. 18 (b) [24]-[26]. The larger external resistance causes a larger IR_{drop} voltage, and thereby resulting in a larger biasing current I_{DROP} . Therefore, the delay time of the delay line circuit is inversely proportional to the IR_{drop} voltage. That is a large voltage IR_{drop} voltage can be interpreted as a big digital number and vice versa. Therefore, the delay-line ADC can

output a different digital code for representing the external resistance according to the various IR_{drop} voltages. The reference shift circuit then increases the reference V_{REF} to V_{REFC} according to the 9-bit digital code.

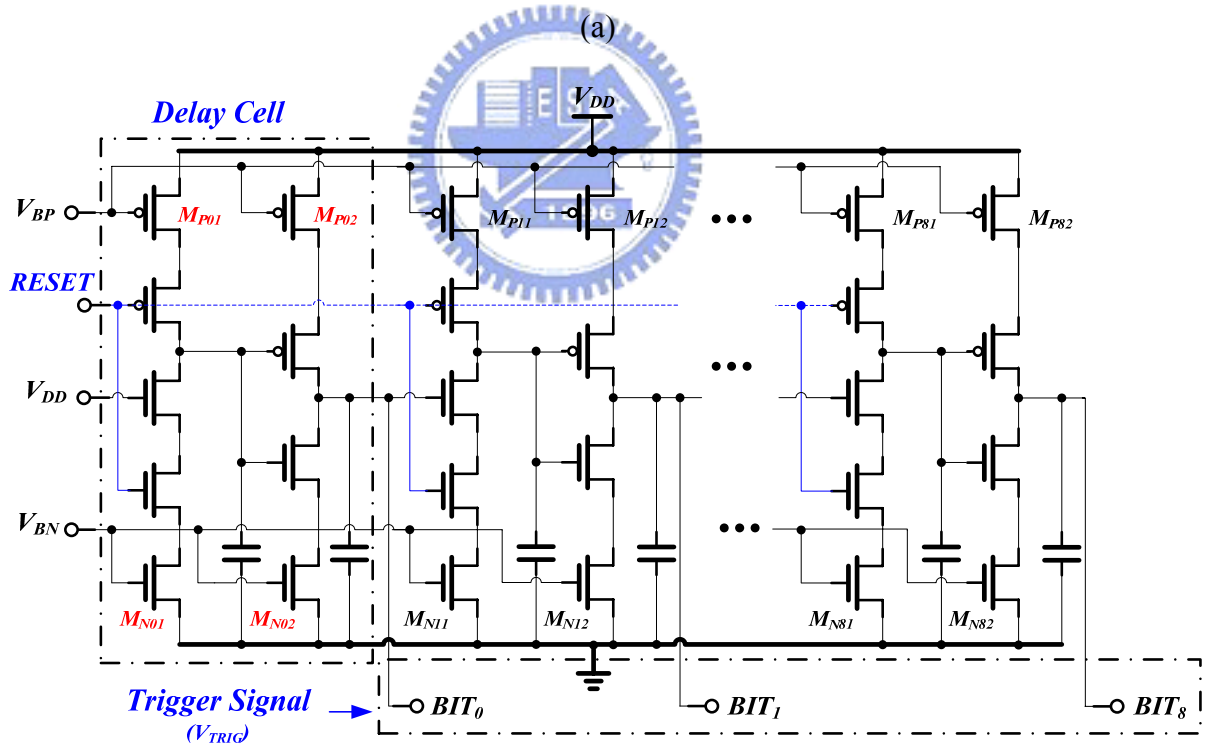
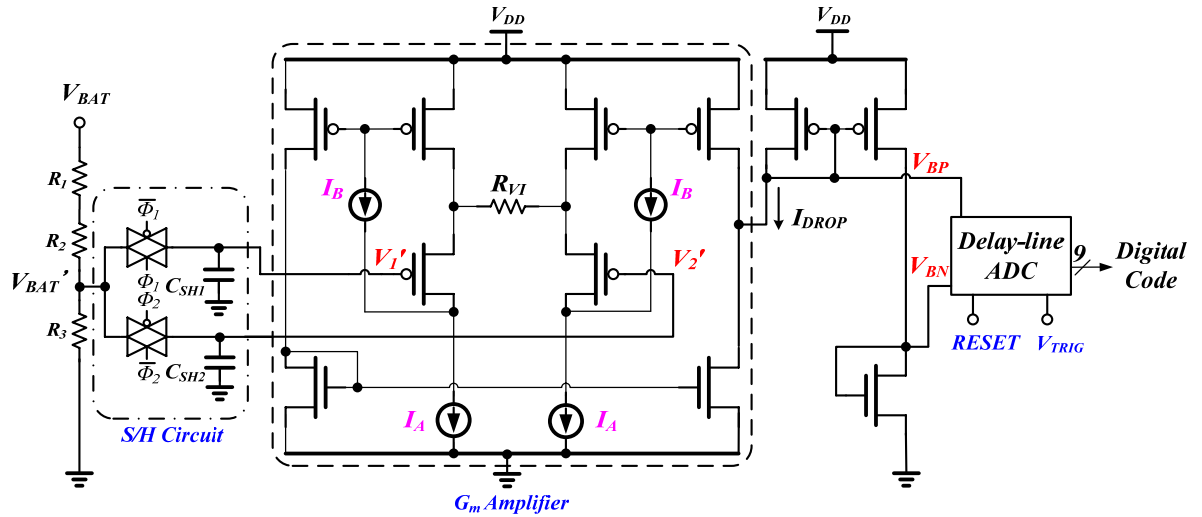


Fig. 18. (a) The schematic of the circuit of external resistance detector with an on-chip sample-and-hold circuit. (b) The schematic of the delay line circuit.

The simulation results of the sample and hold circuit are shown in Fig. 19 and Fig. 20. Fig. 19 is the waveform of V_{BAT}' and V_I' , and V_I' is pre-designed to be sampled when the V_{BAT}' is 2V. The pass transistors are controlled by the signal Φ_I and the cap, C_{SHI} reserves the value, 2V.

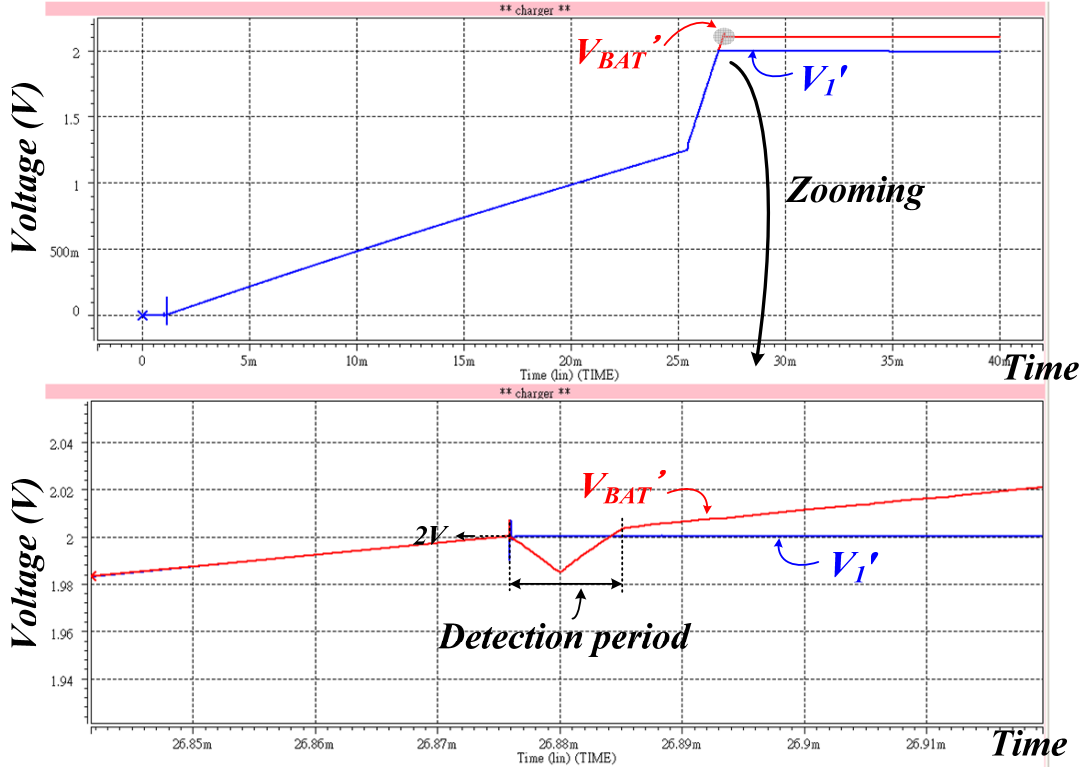
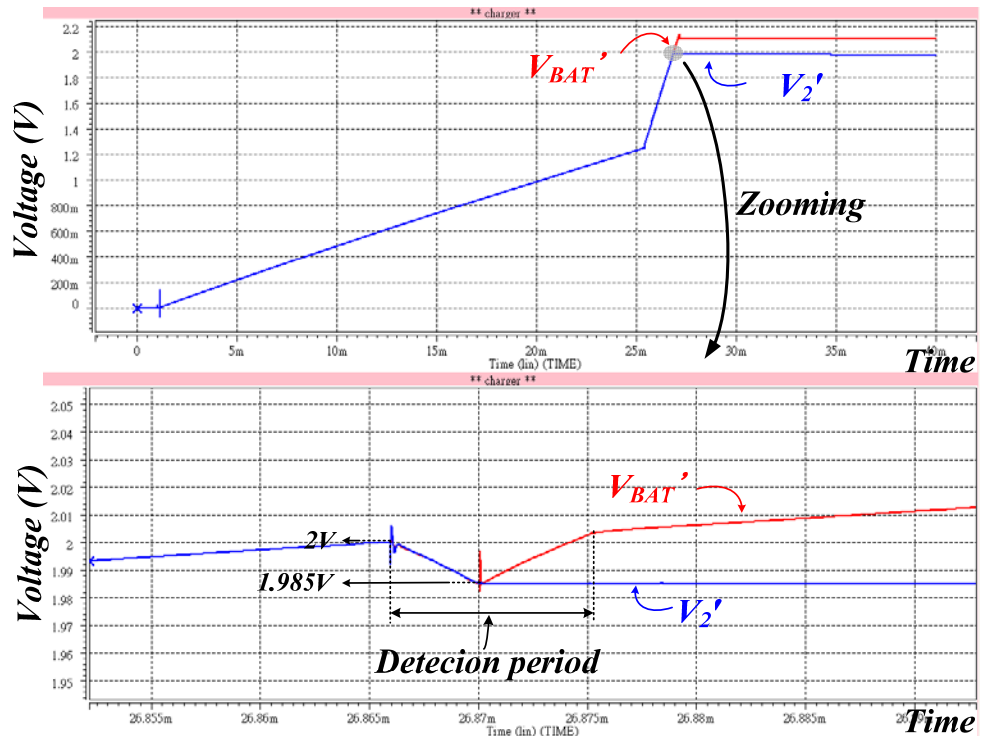
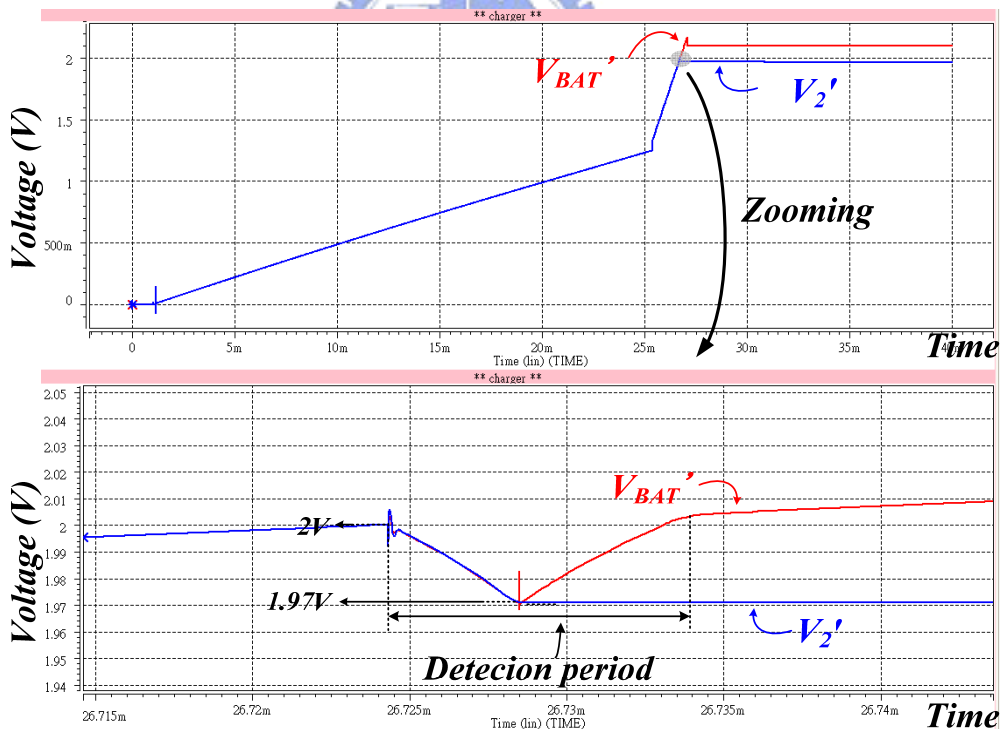


Fig. 19. The waveform of V_{BAT}' and V_I' during the detection period

Fig. 20(a) and Fig. 20(b) are the voltage V_{BAT}' and V_2' of S/H circuit under the condition that $R_{pack}=150m\Omega$ and $300m\Omega$ respectively. Referring to the zooming vision, it is clear that the voltage on the storage capacitance, C_{SH2} could follow the value of V_{BAT}' and the voltage of that at time t_3 referring to Fig. 15 is reserved precisely. Referring to equation (12), since the values of V_I' and V_2' are half of that of V_I and V_2 , the voltage of V_2' is 1.985V and 1.97V. The circuit could record the voltage of V_I' and V_2' and send both the two signals to *Gm-Amplifier* to acquire the current proportional to the differential voltage of that.



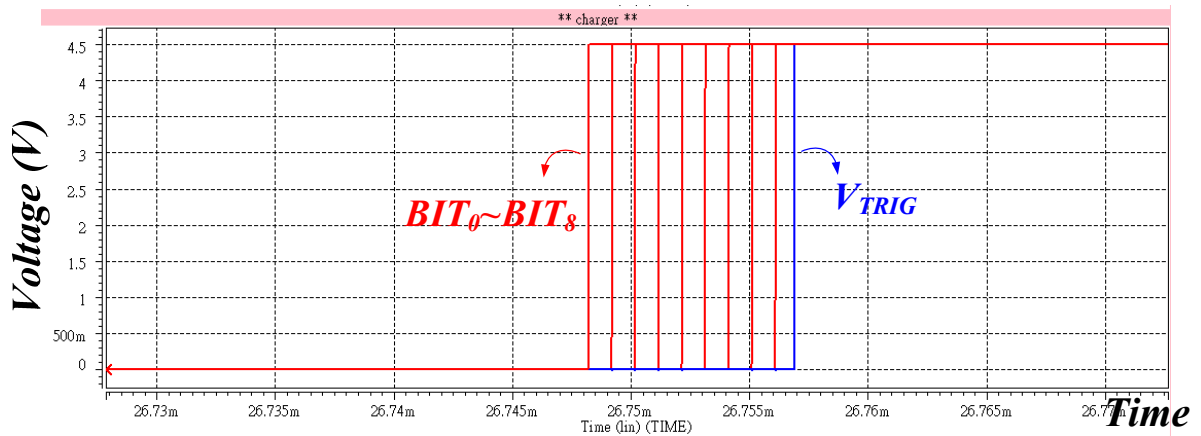
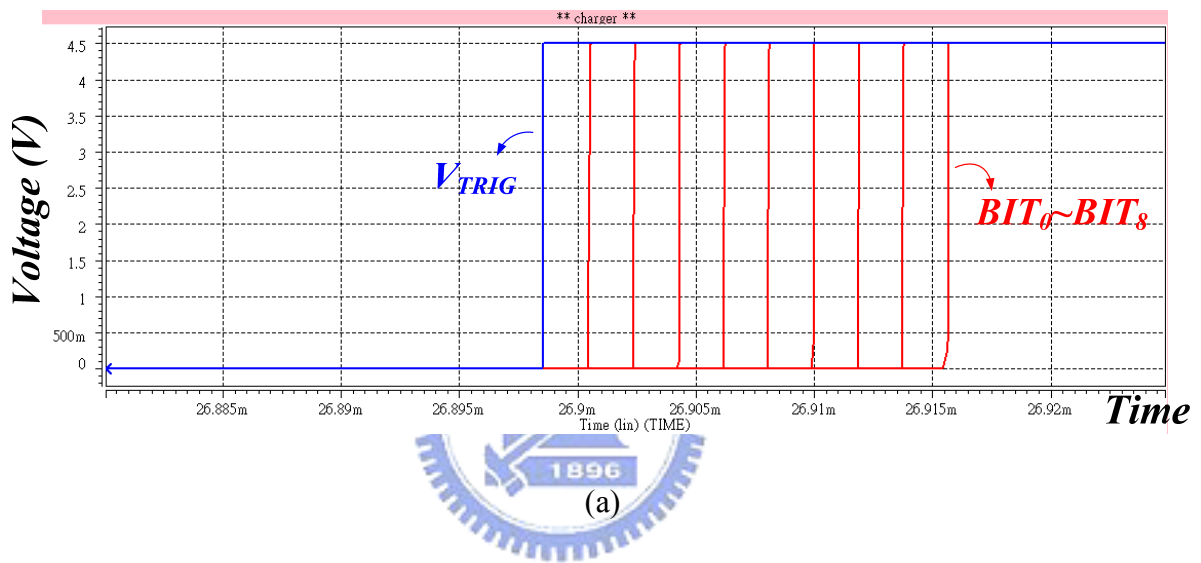
(a)



(b)

Fig. 20. The waveform of V_{BAT}' and V_2' during the detection period, (a) $R_{pack}=150m\Omega$, (b) $R_{pack}=300m\Omega$

The function of the delay line circuit is shown in Fig. 21. The circuit sends the voltage level of digital code from BIT_0 to BIT_8 when the control signal V_{TRIG} is asserted. When the external resistance is $150\text{m}\Omega$, the digital bits are all low and the bits are all high when the resistance is $300\text{m}\Omega$. Besides, the simulation shows that the delay time of each bit is different since the different I_{DROP} . Referring to equation (14), the delay time under the $150\text{m}\Omega$ would be longer than $300\text{m}\Omega$ because of the smaller I_{DROP} .



(b)

Fig. 21. The 9-bit digital code of the delay line circuit, (a) $R_{pack}=150\text{m}\Omega$, (b) $R_{pack}=300\text{m}\Omega$

3.2.5 The Proposed Reference Shift Circuit

After the estimation of the external resistance of the Li-Ion battery pack system, a 9-bit digital code generated by the external resistance detector is sent to the reference shift circuit to add the incremental voltage V_{INC} to the V_{REF} according the value of the digital number, which is converted by the delay-line ADC in Fig. 18 (b). Referring to Fig. 22, the current, I_0, I_1, \dots, I_8 and I_{base} are determined by the value of the voltage V_{SET}' . According to the related documents about Li-Ion cell battery, the external resistance of the Li-Ion battery pack may vary from 150m Ω to 300m Ω .

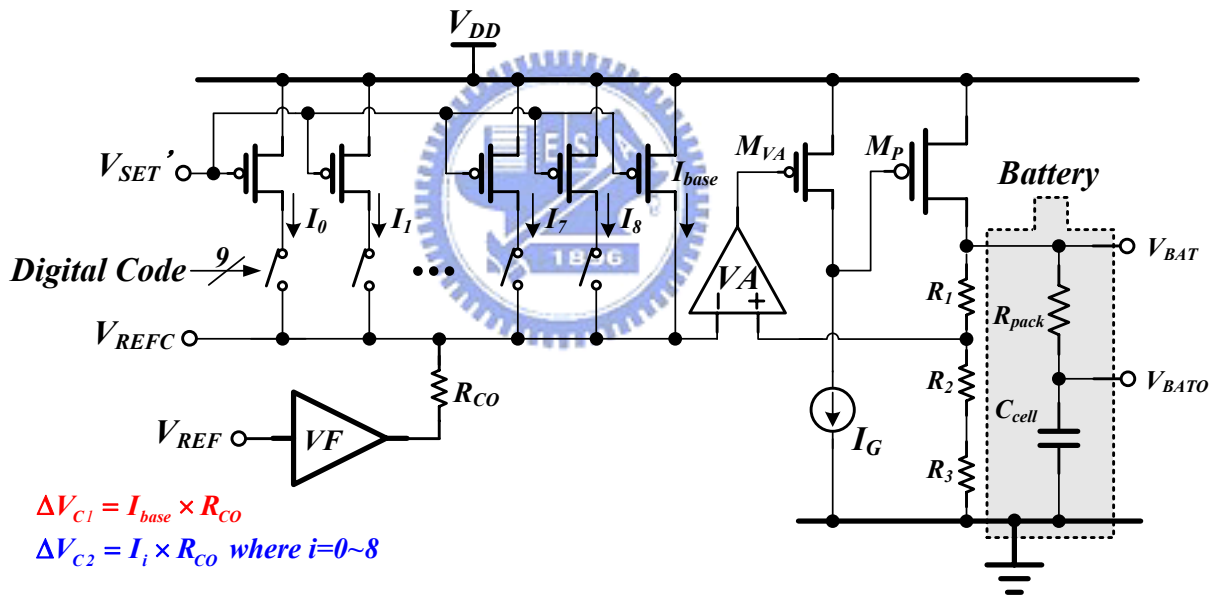


Fig. 22. The reference shift circuit generates the BRC reference voltage V_{REF}' by adding the increment voltage V_{INC} to the original reference voltage V_{REF} .

Assuming that the minimum external resistance is 150m Ω , the needed minimum compensation current is the base current I_{base} , which flows through the resistor R_{CO} and decides the minimum new reference voltage V_{REFC} . The minimum value of the reference voltage V_{REFC} is expressed as (15).

$$V_{REFC(min)} = V_{REF} + (I_{base} \times R_{CO}) = V_{REF} + (150 \text{ m}\Omega) \times I_{CHRG} \times \frac{R_2 + R_3}{R_1 + R_2 + R_3} = V_{REF} + \Delta V_{C1} \quad (14)$$

The value of the voltage V_{ADD} is used to compensate the variation of the external resistance ranged from 150m Ω to 300m Ω . The value of the voltage V_{ADD} can be expressed as (16). Finally, the incremental voltage V_{INC} for compensating the reference voltage is equal to the summation of the voltage ΔV_{C1} and the voltage V_{ADD} .

$$V_{ADD} = \sum_{i=0}^N I_i \times R_{CO} = \left[\frac{N+1}{9} \right] \times I_{CHRG} \times \left(150 \text{ m}\Omega \times \frac{R_2 + R_3}{R_1 + R_2 + R_3} \right) = (N+1) \times \Delta V_{C2} \quad (15)$$

The value of N is from 0 to 8. The corresponding compensating voltages due to different digital codes are listed in TABLE IV. Because the assumption of the smallest external impedance is 150m Ω , ΔV_{C1} compensates the fundamental IR-drop of battery pack system that is referred to equation (15). The current I_0, I_1, \dots, I_8 and I_{base} are flowing through the resistor, R_{CO} to generate the compensate voltage drop. The values of current I_0, I_1, \dots, I_8 and I_{base} are controlled by the value of the voltage V_{SET} . Thus, the values of these currents are gradually decreased to zero when the voltage V_{SET} is decreased to zero due to the decreasing current of the transistor M_{CS} at the CV stage. As a result, the incremental voltage V_{INC} will be smoothly decreased to zero. The reference voltage returns to the original value at the CV stage without affecting the rated full charge voltage.

TABLE IV

THE CORRESPONDING VALUES TO THE VOLTAGE, V_{INC} OF DISTINCT EXTERNAL RESISTANCE,

R_{PACK}

R_{pack} (m Ω)	Digital Code	V_{INC} (mV)	V_{REFC} (V)	
150.00	00000000	1	45	2.545
166.67	00000001	1	50	2.550
183.00	00000011	1	55	2.555
200.00	00000111	1	60	2.560
216.67	00001111	1	65	2.565
233.00	00011111	1	70	2.570
250.00	00111111	1	75	2.575
266.67	01111111	1	80	2.580
283.00	01111111	1	85	2.585
300.00	11111111	1	90	2.590

As shown in Fig. 23 and Fig. 24, the voltage of V_{REFC} is shifted to the specified value. The Fig. 23 shows the compensated V_{REFC} when the 9-bit digital code is 000000001. Referring to equation (15), the minimum value of the reference voltage is 2.545V. During the CV stage of the charging process, the compensated V_{REFC} returns to its original value, 2.5V.

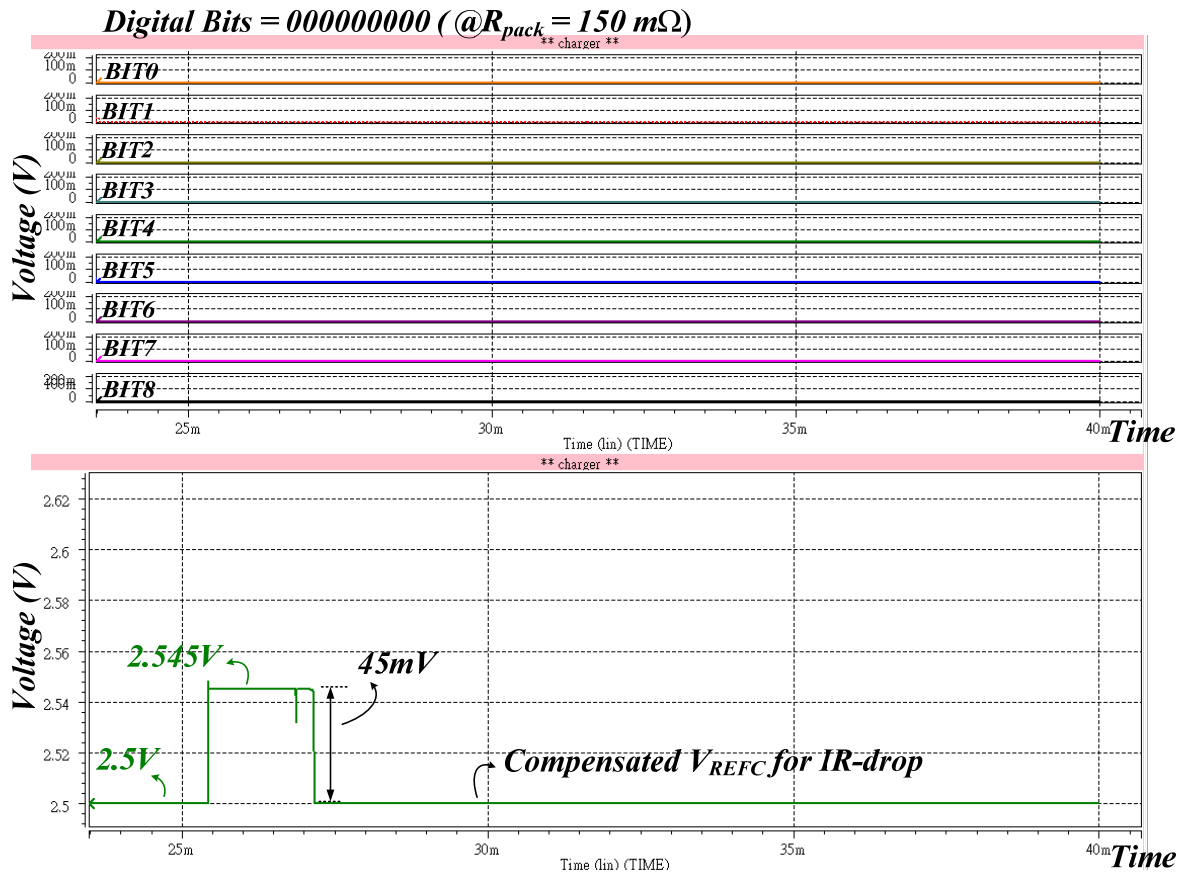


Fig. 23. The waveform of the digital bits, 000000001 and compensated V_{REF} for IR-drop

Fig. 24 shows the compensated V_{REFC} corresponding to the 9-bit digital code, 111111111. The external resistance is larger than 300m Ω and the BRC technique would shift the reference voltage to the max degree to achieve longer CC stage. The max value of V_{INC} is calculated by equation (15), (16) and the number of N is 8. That is the V_{INC} under the resistance of 300m Ω is 2.59V. Similarly, the compensated V_{REFC} is decreased to zero gradually to diminish the effect at CC stage.

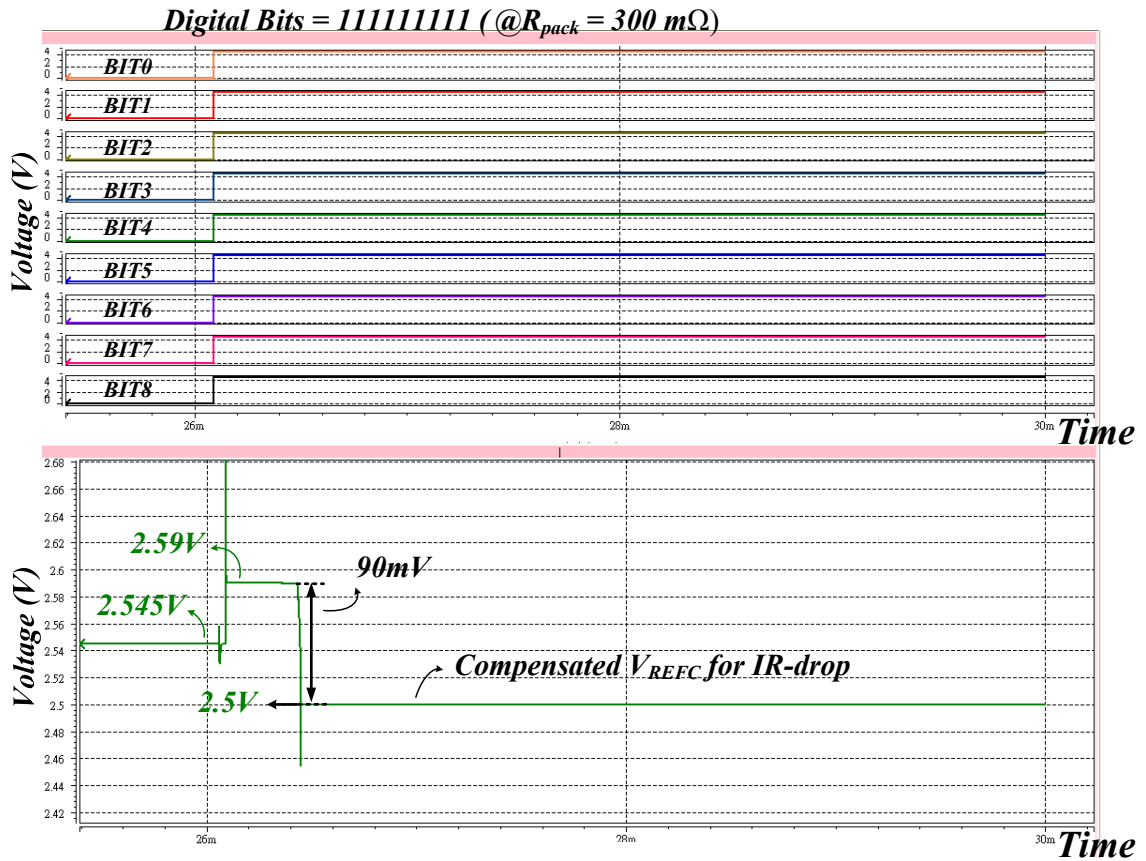


Fig. 24. The waveform of the digital bits, 111111111 and compensated V_{REF}' for IR-drop

After the implementation the proposed charger with the BRC technique, the period of the CC stage can be extended to charge much more energy to the Li-Ion battery cell and the over-charge problem also can be avoided. The most important advantage if the BRC technique is that the IR-drop of the external resistance could be compensated well to fasten the charging process but not violate the original charging system.

3.3 The Whole Circuit Simulation of the Charger with BRC technique

The Fig. 25 shows the simulation result of the voltage level of V_{BAT} and the charging current. From the waveform of the voltage variation, it is clear that the compensated voltage, V_{BATO} reaches the rated voltage earlier than the original one. The shift reference voltage makes the charger stays in CC stage for longer time. After the battery reaches the rated voltage, the reference voltage decreases to the original designed value dynamically and regulate the cell in 4.2V. From the current comparison scheme, the time of degrading current after compensation is shorter than that of uncompensated one. It implies that the greater part of the energy is stored during the CC stage and only the few part of the energy supplied in CV stage.

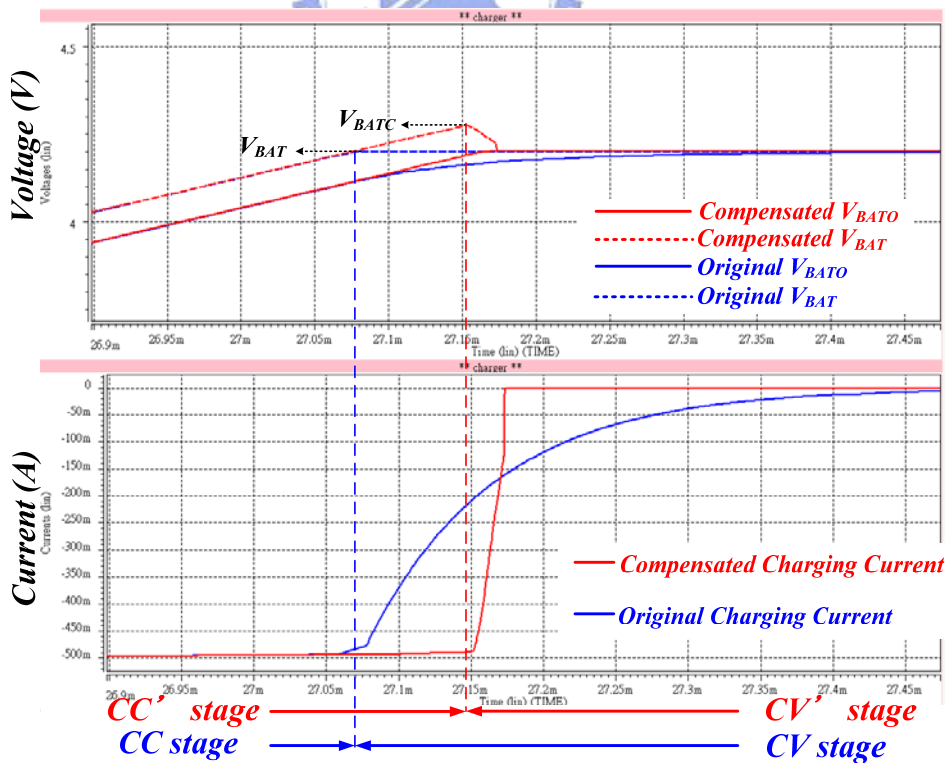


Fig. 25. The whole circuit simulation of the charger with BRC technique

Chapter 4

The Environmental Set-up and the Measurement Results of the Charger with BRC

The Chapter 4 illustrates the experimental result of the charger with the BRC technique. This Chapter is divided into three sections. The section 4.1 introduces the specification and chip micrograph and the demonstration diagram of the proposed charger with BRC technique. The section 4.2 is the measurement results of the charger.

4.1 The Environmental Set-up and Chip Micrograph of the BRC Charger

The proposed charger with the BRC technique was implemented in TSMC 2P4M 0.35- μm CMOS technology. The input range of the power supply is from 4.5v to 6.5v, and the rated full-voltage of the battery is 4.2V. The threshold voltages of nMOSFET and pMOSFET are 0.55 V and 0.65 V, respectively. TABLE V lists the detailed specifications of the proposed charger.

TABLE V:

SPECIFICATIONS OF THE PROPOSED CHARGER WITH THE BRC TECHNIQUE

V_{DD}	4.5 V~6.5 V
C_{cell}	10000 μF
R_{pack}	150 m Ω ~ 300 m Ω
V_{r1}	0.15 V
V_{r2}	0.9 V
V_{r3}	1.5 V
R_{SET}	3.0 K Ω
V_{REF}	2.5 V
V_{FULL}	4.2 V
V_1	4.0 V
V_1'	2.0 V
I_{CHRG1}	500mA
I_{CHRG2}	300mA

The set-up of the test chip is shown in Fig. 26. The pin of EN_BRC can be set to low to turn off the BRC technique system. The supply voltage of charger is 5V and the fully charged voltage V_{FULL} is 4.2V. In order to emulate the external resistance of the battery pack system, one resistor R_{pack} of 300 m Ω is used to stand for the external resistance. Furthermore, in order to monitor the charging process within a short period, one large capacitor C_{CELL} of 10000 μF is used to emulate the large capacity of the Li-Ion battery.

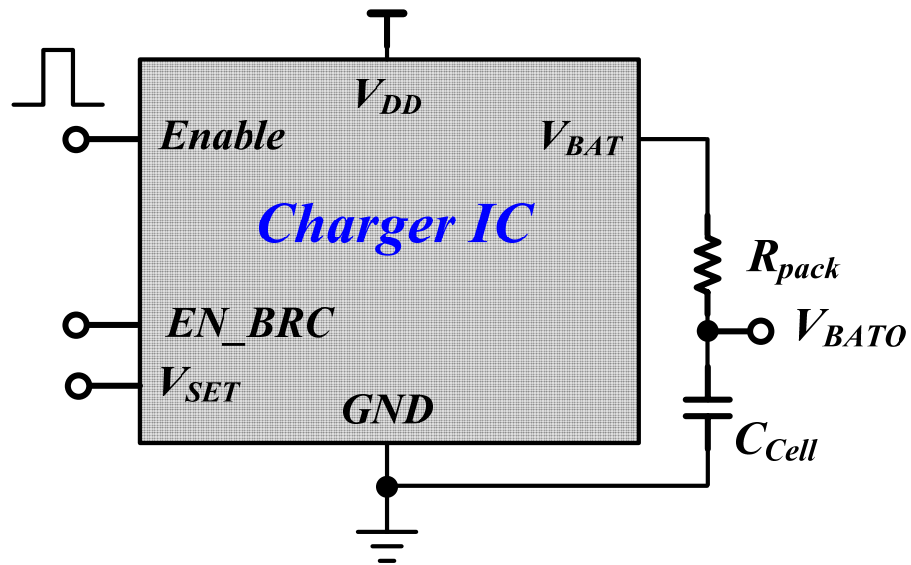


Fig. 26. The estimation set-up of the proposed charger.

Fig. 27 is chip micrograph of the proposed charger with BRC technique. The silicon area is $1300 \times 850 \mu\text{m}^2$. The chip was implemented in TSMC 2P4M 0.35- μm CMOS technology.

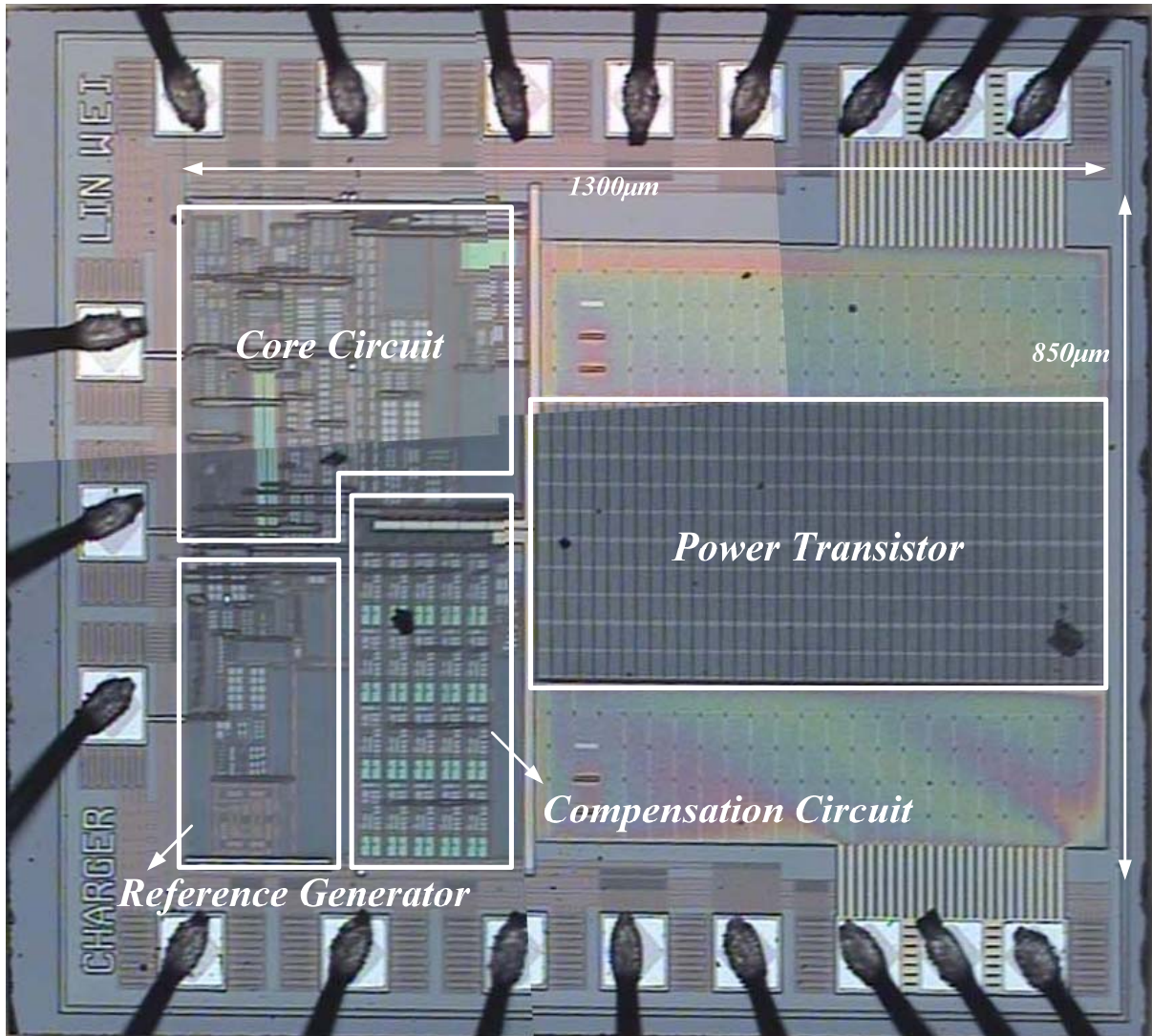


Fig. 27. Chip micrograph.

4.2 The Measurement Results of the Charger

As illustrated in Fig. 28, the waveform of the battery cell V_{BATO} is presented based on the smooth control circuit. The enable signal is used to control the charging process. By adopting the current control method in the design of CA amplifier, the charger smoothly switches from the CC stage to the CV stage without any iteration between the CC and CV stages. The current loop, which is composed of the CA and MA amplifiers, is gradually turned off. The charger becomes a linear regulator after the voltage loop, which is constituted by the VA amplifier, controls the charger. Besides, the common usage range of the Li-Ion battery is from 2.5V to 5V. When battery is discharged to 2.5V, the stored energy of the battery is empty and needed to be charged. That is, the battery is usually charged from about 2.5V.

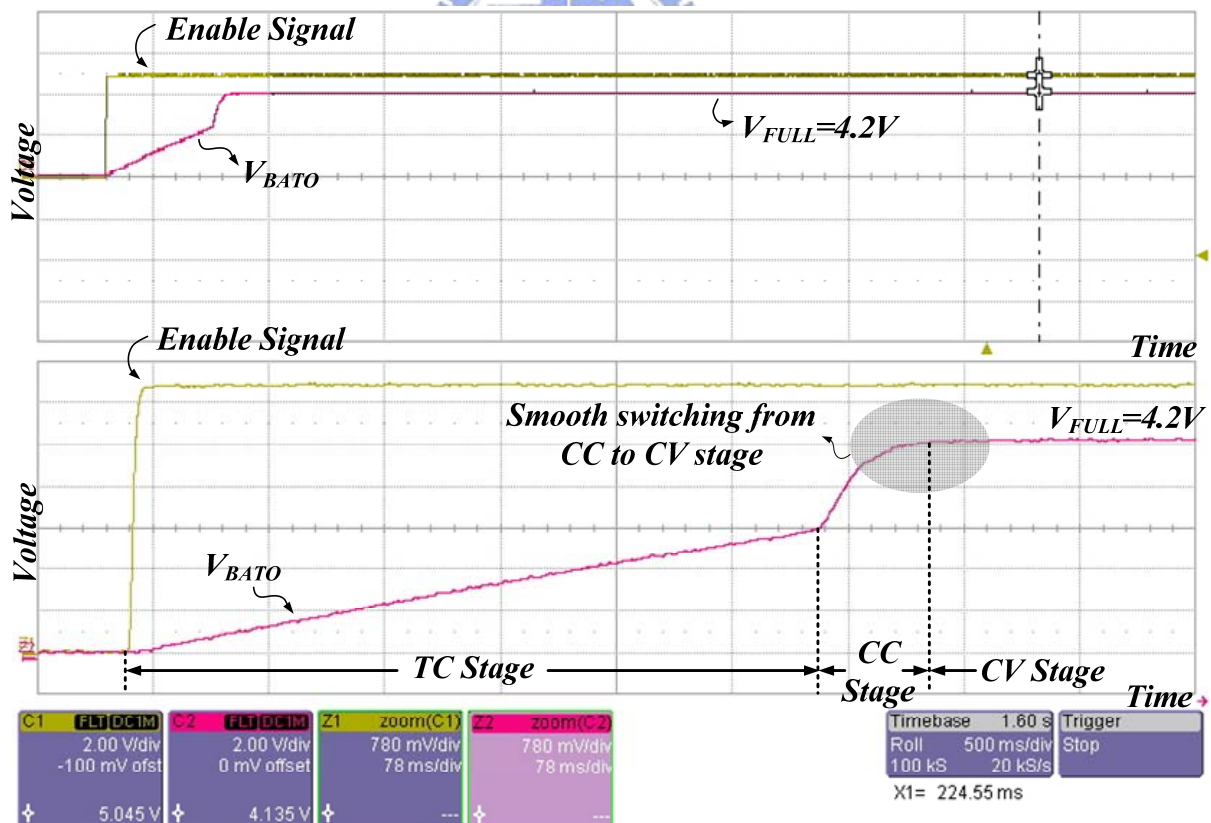


Fig. 28. The smooth charging waveform from the CC to CV stage achieved by the analogy method.

Since the output capacitor is $10000\mu\text{F}$, it is easy to find out the charging time of the TC stage is 500ms . In Fig. 29, the estimated result is similar to that got from the calculation. Furthermore, the period of the CC and CC' stages are 22ms and 32ms , respectively. The period of the CC stage is extended to about 40% that of the original charger without the BRC technique.

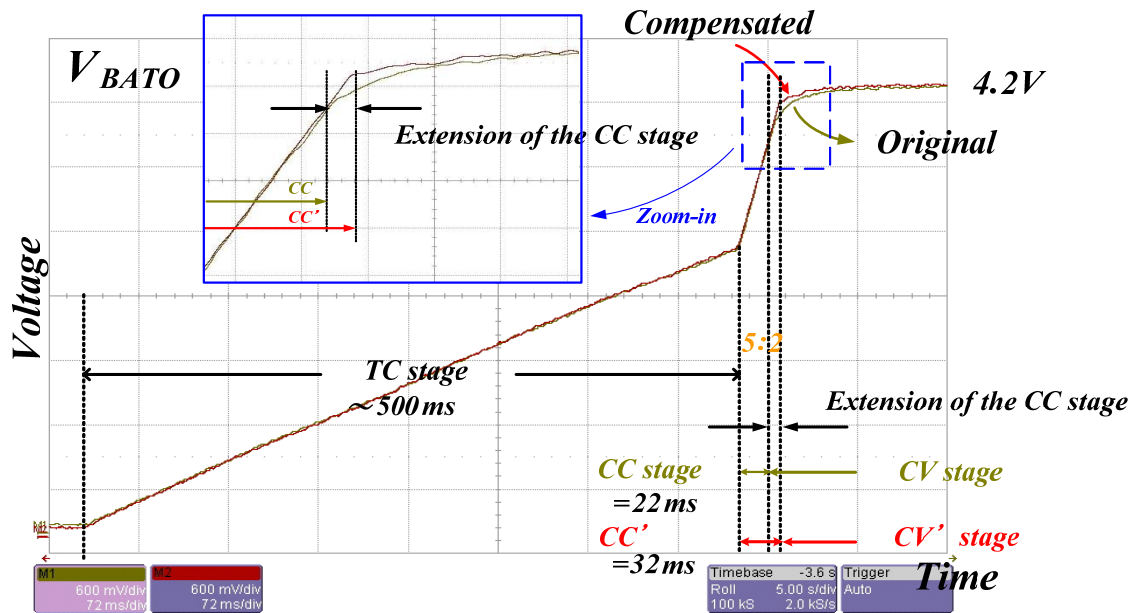


Fig. 29. The waveforms of the voltage V_{BATO} w/i and w/o the BRC technique. The CC stage of the original design is extended to the CC' stage of the BRC design.

Due to the external resistance is $300\text{m}\Omega$, the digital number of the detector is 111111111. Then, the reference-shift circuit adds the max shift-voltage to the reference voltage V_{REF} for compensating the IR-drop voltage. Thus, the voltage V_{BATO} at the Li-Ion cell can reach the specific voltage, 4.2V more quickly than that of the original design without the BRC technique. From the zoom-in window in Fig. 29, the voltage V_{BATO} can be rapidly raised to 4.2V due to the extension of the CC stage.

In Fig. 30, the IR-drop voltage exists between the voltages V_{BATO} and V_{BAT} . The period of the constant current stage can be extended from the CC stage to the CC'' stage since the value of the compensated V_{BATC} is larger than that of the original V_{BAT} .

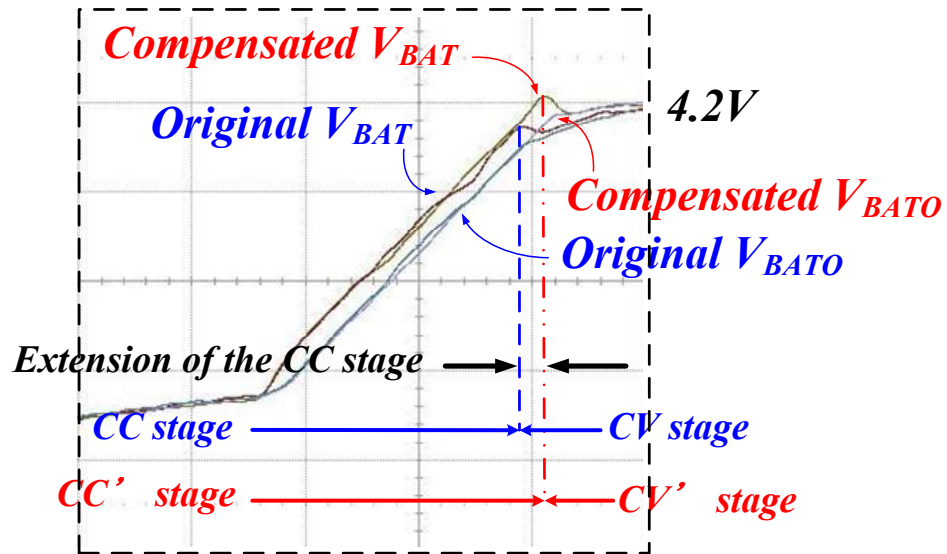


Fig. 30. The waveforms of the voltages V_{BAT} and V_{BATO} w/i and w/o the BRC technique. The voltages of the compensated V_{BAT} and V_{BATO} are got from the BRC technique.

The waveform of the voltage V_{SET} is shown in Fig. 31. During the detection period, the voltage, V_{SET} is pulled low to 0.9V for a short time and back to 1.5V. The detection period is 0.5ms in Fig. 31. During the detection period, the charger acquires the sufficient information of the external resistance of the battery pack system to compensate the IR-drop voltage.

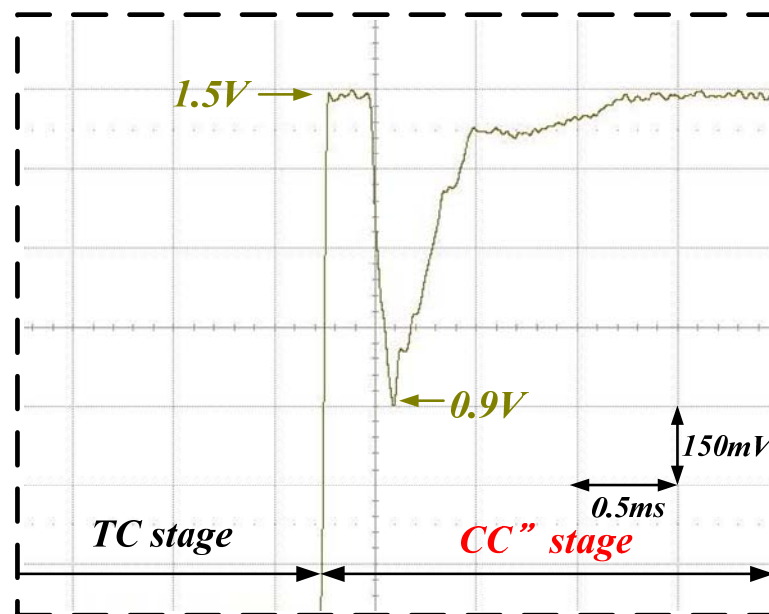


Fig. 31. The waveform of the voltage V_{SET} during the detection period.

Chapter 5

Conclusions and Future Works

In this chapter, the conclusions of the proposed circuit are shown in section 5.1. At the end, the future works of the charger with BRC technique are shown in section 5.2.

5.1 Conclusions

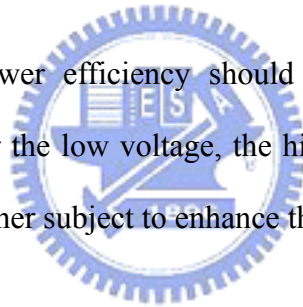
This paper proposed a smooth transition method from the CC stage to the CV stage for the Li-Ion charger. Due to the external parasitic resistance of the Li-Ion battery pack system, the charger circuit switches from the CC stage to the CV stage without fully charging the cell to the rated voltage value. The longer the charging time is due to the degrading current at the CV stage. Therefore, the charger circuit has the new BRC technique to speed up the charging time of the Li-Ion battery. The BRC technique can dynamically estimate the external resistance of the battery pack system to extend the period of the CC stage for achieving a fast charging response. Experimental results show the period of the CC stage can be extended to about 40% that of the original design. That is the charger with the BRC technique can smoothly transit from the CC stage to the CV stage and have the fast charging performance.

5.2 Future Works

This paper proposed a novel technique of the fast-speed charging charger. The charger can detect the external resistance of the battery pack system automatically and compensate the voltage drop to shorten the charging process. However, there are some disadvantages of the conditional charger that can be improved.

First, the temperature is the key factor of the battery charger. The external resistance could vary under the different temperature. In the proposed design, the detection of the external resistance starts when the battery reaches 4V for the temperature consideration. The temperature-dependent detection circuit could be developed to increase the accuracy of the resistance.

Second, the issue of power efficiency should be considered. When the battery is connected to the charger under the low voltage, the high supply voltage is unnecessary. The dynamic supply voltage is another subject to enhance the performance of the charger.



References

- [1] Linear Technology, LTC1733 data sheet, LTC3440 data sheet
- [2] D. Linden and T. B. Reddy, *Handbook of Batteries*. New York: Mc-Graw-Hill, 2002, ch. 35.
- [3] Min Chen, Gabriel A. Rincón-Mora, “Accurate, Compact, and Power-Efficient Li-Ion Battery Charger Circuit,” *IEEE Trans. Circuits and Systems II*, vol. 53, no. 11, pp. 1180-1184, Nov. 2006.
- [4] Ke-Horng Chen, “Extend the Battery Life by Highly Efficient DC-DC Converters,” *Proceedings of 2004 Taipei Internal Power Forum*, Dec. 2004.
- [5] Chenghui Cai, Dong Du, Zhiyu liu, “Advanced Traction Rechargeable battery System For Cableless Mobile Robot,” *IEEE/ASME International Conference on Advanced Intelligent Mechanics*, vol. 1, pp. 234-239, July. 2003
- [6] Teruo Kodama, Hikari Sakaebe, “Present Status and Future Prospect for National Project on Lithium Batteries,” *Journal of Power Sources*, vol. 81-82, pp. 144-149, Sep. 1999
- [7] M. J. Isaacson, R. P. Hollandsorth, P. J. Giampaoli, F. A. Linkowaky, A. Salim, V. L. Teofilo, “Advanced Lithium Ion Battery Charger” *The Fifteenth Annual Battery Conference on Applications and Advances*, pp. 193-198, Jan. 2000
- [8] Chia-Chun Tsai, Chin-Yen Lin, Yuh-Shyan Hwang, Wen-Ta Lee and Trong- Yen Lee, “A multi-mode LDO-based Li-ion battery charger in 0.35 μ m CMOS Technology,” *IEEE Asia-Pacific Conference on Circuits and Systems*, pp. 49-52, Dec. 2004
- [9] Amir M. Rahimi, “A lithium-ion battery charger for charging up to eight cells,” *IEEE Conference, Vehicle Power and Propulsion*, 2005

- [10] Yuh-Shyan Hwang, Shu-Chen Wang, Fong-Cheng Yang, Jiann-Jong Chen, “New Compact CMOS Li-Ion Battery Charger Using Charge-Pump Techniques for Portable Applications,” *IEEE Trans. Circuits and Systems I*, vol. 54, no. 4, pp. 705-712, April 2007.
- [11] J. Buxton, “Li-Ion battery charging requires accurate voltage sensing,” *Anal. Devices Anal. Dialog.*, vol. 31, no. 2, 1997.
- [12] J. Lopez, M. Gonzalez, J. C. Viera, C. Blanco,” Fast-Charge in Lithium-Ion Batteries for Portable Applications,” *The 26th Annual International Telecommunications Energy Conference (INTELEC)*, Sep. 2004.
- [13] Hari Vaidyanathan, Gopalakrishna Rao ,” Electrical and Thermal Characteristics of Lithium-Ion Cells,” *The Fourteenth Annual Battery Conference on Applications and Advances*, 1999.
- [14] S. Dearborn, “Charging Li-ion batteries for maximum run times,” *Power Electron. Technol. Mag.*, pp. 40–49, Apr. 2005.
- [15] F. Lima, J. N. Ramalho, D. Tavares, J. Duarte, C. Albuquerque, T. Marques, A. Geraldés, A. P. Casimiro, G. Renkema, J. Been, and W. Groeneveld, “A novel universal battery charger for NiCd, NiMH, Li-Ion and Li-Polymer,” in *Proc. Eur. Solid-State Circuits Conf.*, pp. 209–212. 2003.
- [16] Huan-Jen Yang, Han-Hsiang Huang, Chi-Lin Chen, Ming-Hsin Huang, and Ke-Horng Chen, “Current Feedback Compensation (CFC) Technique for Adaptively Adjusting the Phase Margin in Capacitor-Free LDO Regulators,” *51th IEEE Int'l Midwest Symposium on Circuits & Systems*, Aug. 2008.
- [17] Yung-Hsin Lin, Kuo-Lin Zheng, and Ke-Horng Chen, “Power MOSFET Array for Smooth Pole Tracking in LDO Regulator Compensation,” *50th IEEE Int'l Midwest Symposium on Circuits & Systems/5th IEEE Int'l Northeast Workshop on Circuits & Systems*, pp. 554-557, Aug. 2007.

- [18] M. F. M. Elias, K. M. Nor, N. A. Rahim, A. K. Arof, "Lithium-Ion Battery Charger for High Energy Application," Power Engineering Conference, pp. 283-288, Dec. 2003.
- [19] Roland Saint-Pierre, "A Dynamic Voltage-Compensation Technique for Reducing Charge Time in Lithium-Ion Batteries," *The Fifteenth Annual Battery Conference on Applications and Advances*, pp. 179-184, Jan. 2000.
- [20] P. Allen and D. Holberg, *CMOS Analog Circuit Design*, New York: Oxford University Press, 2002
- [21] Behzad Razavi, *Design of Analog CMOS Integrated Circuits*, New York: Mc-Graw-Hill, 2001
- [22] J. Ramirez-Angulo, R. G. Carvajal, A. Torralba, J. Galan, A. P. Vega-Leal, and J. Tombs, "The Flipped Voltage Follower: A useful cell for low-voltage low-power circuit design," *IEEE Trans. Circuits and Systems I*, vol.52, no. 7, pp. 1276-1291, July 2005
- [23] Ivan Padilla and Jaime Ramirez-Angulo, Ramon G. Carvajal, Antonio Lopez-Martin, "Highly Linear V/I Converter with Programmable Current Mirrors, *IEEE International Symposium on Circuits and Systems (ISCAS)*, pp. 941-944, May 2007.
- [24] Hong-Wei Huang, Ke-Horng Chen, and Sy-Yen Kuo, "Dithering Skip Modulation, Width and Dead Time Controllers in Highly Efficient DC-DC Converters for System-on-chip Applications," in *IEEE Journal of Solid-State Circuits*, pp. 2451-2465, Nov. 2007.
- [25] Hong-Wei Huang, Hsin-Hsin Ho, Ke-Horng Chen, and Sy-Yen Kuo, "Dithering Skip Modulator with a Novel Load Sensor for Ultra-wide-load High-Efficiency DC-DC Converters," *International Symposium on Low Power Electronics and Design – 2006*, pp. 388-393, Oct. 2006.
- [26] Ke-Horng Chen, Li-Ren Huang, Hong-Wei, Huang, Sy-Yen Kuo, US Patent 20070247346(2007), "Delay Line, Analog-To-digital Converting Device And Load-Sensing Circuit Using the Same".

ISSUED PAPER LIST

- [1] Chia-Hsiang Lin, Chi-Lin Chen, Yu-Huei Lee, Shih-Jung Wang, Chun-Yu Hsieh, Hong-Wei Huang, Ke-Horng Chen, "Fast Charging Technique for Li-Ion Battery Charger," *The Fifteenth IEEE International Conference on Electronics, Circuits, and Systems*, Sep. 2008
- [2] Chia-Hsiang Lin, Hong-Wei Huang, Ke-Horng Chen, "Built-in Resistance Compensation (BRC) Technique for Fast Charging Li-Ion Battery Charger," *The Thirtieth IEEE Custom Integrated Circuits Conference*, Sep. 2008
- [3] Hong-Wei Huang, Chia-Hsiang Lin, Ke-Horng Chen, "High-Performance Low-Dropout Regulator Achieved by Fast Transient Mechanism," *The Thirty-fourth European Solid-State Circuits Conference (ESSCIRC)*, Sep. 2008
- [4] Hong-Wei Huang, Chia-Hsiang Lin, Ke-Horng Chen, "Low-Dropout Regulators with Adaptive Reference Control and Dynamic Push-Pull Techniques for Enhancing Transient Performance," *The IEEE Transactions on Power Electronics*,

